Advanced analytical methodologies in Alzheimer's disease drug discovery

(Article begins on next page)

08 June 2024

Advanced analytical methodologies in Alzheimer's disease drug discovery

Angela De Simone [a], Marina Naldi [b,c], Daniele Tedesco [b], Manuela Bartolini [b],

Lara Davani [a], Vincenza Andrisano [a]

[a] *Department for Life Quality Studies, Alma Mater Studiorum – University of Bologna, Rimini, Italy.*

[b] *Department of Pharmacy and Biotechnology, Alma Mater Studiorum – University of Bologna, Bologna, Italy.*

[c] *Center for Applied Biomedical Research (C.R.B.A.), Sant'Orsola-Malpighi Hospital, Bologna, Italy.*

Abstract

Despite the constant progress in the understanding of the etiopathogenesis of Alzheimer's disease (AD) over the last 50 years, just four long-standing drugs are currently used for AD therapy. This article reviews the analytical methodologies developed and applied in the last five years to address the early-stage tasks of the AD drug discovery process: the fast selection of active compounds (hits) and the comprehension of the ligand binding mechanism of the compound chosen to be the lead in the forthcoming development. The reviewed analytical methodologies face the most investigated pharmacological protein targets (amyloids, secretases, kinases, cholinesterases) and specific receptor- and enzyme-mediated effects in neurotransmission, neuroprotection and neurodegeneration. Some of these methodologies are noteworthy for their use in middle/high-throughput screening campaigns during hit selection (e.g. surface plasmon resonance biosensing, fluorescence resonance energy transfer assays), whereas some others (circular dichroism and nuclear magnetic resonance spectroscopies, ion mobility–mass spectrometry) can provide in-depth information about the structure, conformation and ligand binding properties of target proteins.

Keywords

Abbreviations

2D HSQC: two-dimensional heteronuclear single quantum coherence;

Aβ: amyloid beta peptide;

ABAD: amyloid beta-binding alcohol dehydrogenase;

AChE: acetylcholinesterase;

AD: Alzheimer's disease;

ADMET: absorption, distribution, metabolism, excretion, and toxicity;

AFM: atomic force microscopy;

APP: amyloid precursor protein;

ATD: arrival time distribution;

ATP: adenosine triphosphate;

BACE1: beta-secretase, beta-site amyloid precursor protein-cleaving enzyme 1;

CD: circular dichroism;

CE: capillary electrophoresis;

CLSM: confocal laser-scanning microscopy;

CORM: carbon monoxide-releasing molecule;

CypD: cyclophilin D;

DAG: diacylglycerol;

DEAC: diethylaminocoumarin;

DMSO: dimethyl sulfoxide;

ECD: electronic circular dichroism;

EDTA: ethylenediaminetetraacetic acid;

EGCG: epigallocatechin gallate;

ESI: electrospray ionization;

FCS: fluorescence correlation spectroscopy;

Fl-δC1b: fluorescein-labeled δC1b domain;

FRET: fluorescence resonance energy transfer;

FT: Fourier-transform;

GLP-1R: glucagon-like peptide 1 receptor;

GSK-3α: glycogen synthase kinase 3α;

GSK-3β: glycogen synthase kinase 3β;

GSM: glycogen synthase muscle;

HEPES: 4-(2-hydroxyethyl)-1-piperazineethanesulfonic acid;

HSA: human serum albumin;

2

HS-AFM: high-speed atomic force microscopy;

HR-MS: high-resolution mass spectrometry;

HTS: high throuput screening;

IAPP: islet amyloid polypeptide;

IMS: ion mobility spectrometry;

IMER: immobilized enzyme reactor;

IR: infrared;

LC: liquid chromatography;

LILBID: laser-induced liquid bead ion desorption;

LSM: laser-scanning microscopy;

MALDI: matrix-assisted laser desorption/ionization;

MAP-2: microtubule-associated protein 2;

MB: methylene blue;

mPTP: mitochondrial permeability transition pore;

MS: mass spectrometry;

MTDL: multitarget-directed ligand;

NAD: nicotinamide adenine dinucleotide;

NBD: nitrobenzoxadiazole;

NF-κB: nuclear factor kappa-light-chain-enhancer of activated B cells;

NMDA: *N*-methyl-D-aspartate;

NMR: nuclear magnetic resonance;

NOE: nuclear Overhauser effect;

PB: phosphate buffer;

PBS: phosphate buffered saline;

PKC: protein kinase C;

PrP^C: cellular prion protein;

QTOF: quadrupole time-of-flight;

RAGE: receptor for advanced glycation end-products;

SAR: structure-affinity relationship;

SEM: scanning electron microscopy;

SIRT1: sirtuin 1;

SOFAST-HMQC: selective optimized-flip-angle short-transient heteronuclear multiple quantum coherence;

SPR: surface plasmon resonance;

s.s.e.: secondary structure estimation;

STD: saturation transfer difference;

TAMRA: 5-carboxytetramethylrhodamine;

TEM: transmission electron microscopy;

ThT: thioflavin T;

TOF: time-of-flight;

Tr-NOESY: transferred nuclear Overhauser effect spectroscopy;

TROSY: transverse relaxation-optimized spectroscopy;

UV-RR: ultraviolet resonance Raman;

UV-Vis: ultraviolet-visible;
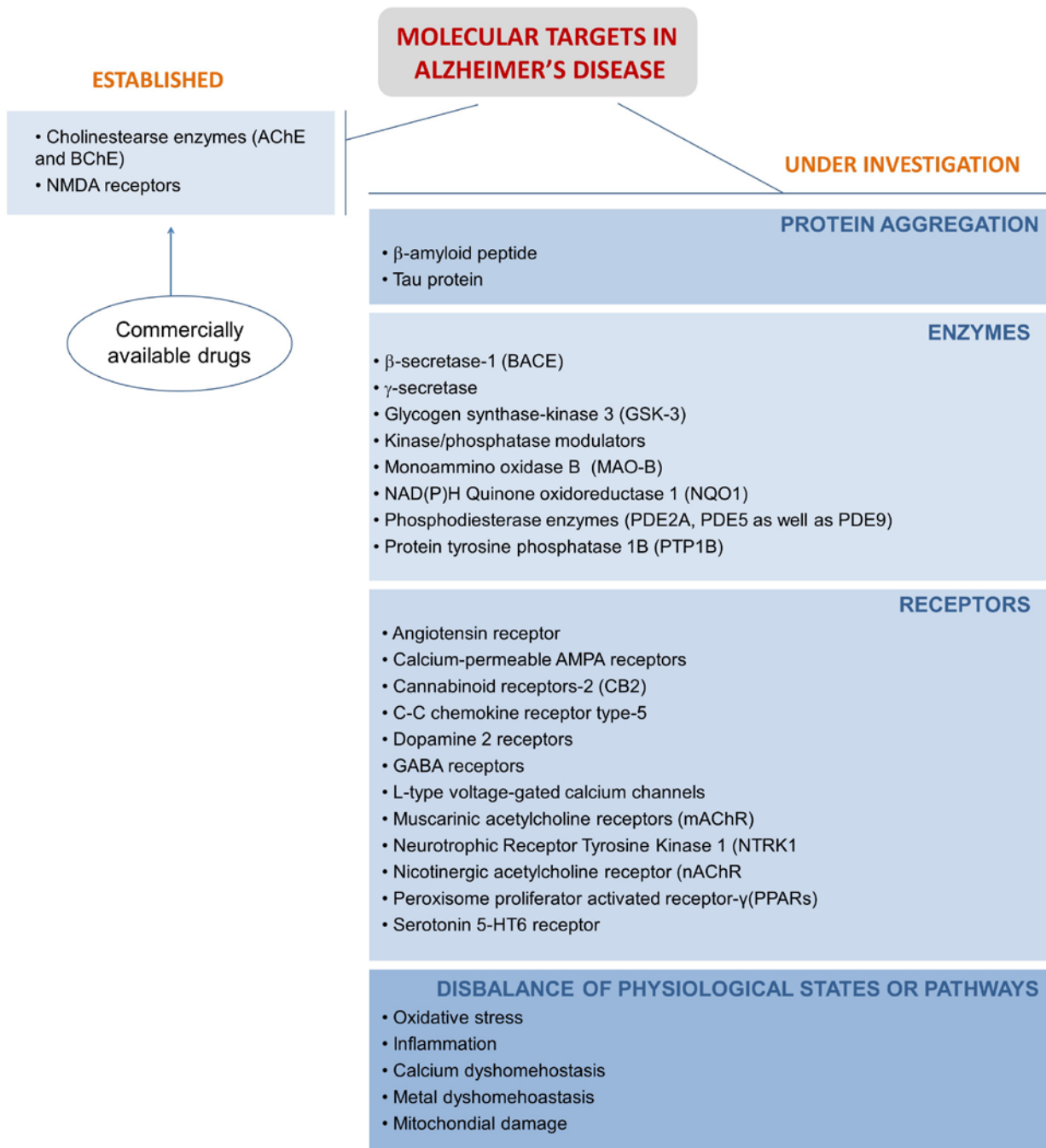
VCD: vibrational circular dichroism.

Table of contents

1. Introduction

Pharmaceutical analysis largely contributes to and eases the drug discovery process by offering suitable tools and methods to assess key parameters, from the identification of biomarkers and the investigation of the absorption, distribution, metabolism, excretion and toxicity (ADMET) of drugs in pre-clinical and clinical studies, up to quality control and validation during drug manufacturing. In recent years, advanced analytical methodologies have been increasingly applied at various stages of early drug discovery (hit identification, structure-properties relationships), with applications spanning from simple *in vitro* assays on single molecules to complex investigations on biological samples. The technological improvements in separation sciences, the advent of soft-impact mass spectrometry (MS) methods and the increasing use of biophysical tools for molecular recognition studies, such as surface plasmon resonance (SPR), ensures accuracy and reproducibility for a wide range of analytes, going from simple organic molecules to biopharmaceuticals, and can strongly assist the drug discovery process. Moreover, the development of automated high-throughput screening (HTS) greatly contributes to hit selection and to the characterization of the mechanism of action of new drug candidates.

In the present review, a selection of analytical approaches developed in the last five years for Alzheimer's disease (AD) drug discovery is provided, mainly focusing on their application in hit selection and in the characterization of the most studied target proteins and their interactions with drug-like molecules. AD is a multifactorial disorder in which genomic alterations, epigenetic abnormalities, cerebrovascular damage and environmental risk factors, joined together, induce a premature and progressive neuronal loss. Statistics recognize AD as the most significant and widespread neurodegenerative disorder. Since the identification of AD by Alois Alzheimer in 1906, the amyloid-tau hypotheses have laid down the basis for drug discovery campaigns with the evidence of amyloid plaques and neurofibrillary tangles in the post mortem brain of patients affected by the disease; however, the drug discovery for AD began in 1984 with the cholinergic hypothesis of memory impairment. Acetylcholinesterase (AChE), catalyzing the hydrolysis of acetylcholine, emerged as a promising target for the discovery of inhibitors capable of temporally restoring the cognitive impairment by increasing neurotransmitter levels in the central nervous system.

During the last 40 years, only five drugs for the treatment of AD have been launched on the market (Figure 1): four cholinesterase inhibitors (tacrine, donepezil, rivastigmine, galantamine; 1993–2000) and one *N*-methyl-D-aspartate (NMDA) receptor antagonist (memantine, approved by the EMA in 2002 and by the FDA in 2003) [1].

MOLECULAR TARGETS IN ALZHEIMER'S DISEASE

ESTABLISHED

- Cholinestearse enzymes (AChE and BChE)
- NMDA receptors

Commercially available drugs

UNDER INVESTIGATION

PROTEIN AGGREGATION
- β-amyloid peptide
- Tau protein

ENZYMES
- β-secretase-1 (BACE)
- γ-secretase
- Glycogen synthase-kinase 3 (GSK-3)
- Kinase/phosphatase modulators
- Monoammino oxidase B (MAO-B)
- NAD(P)H Quinone oxidoreductase 1 (NQO1)
- Phosphodiesterase enzymes (PDE2A, PDE5 as well as PDE9)
- Protein tyrosine phosphatase 1B (PTP1B)

RECEPTORS
- Angiotensin receptor
- Calcium-permeable AMPA receptors
- Cannabinoid receptors-2 (CB2)
- C-C chemokine receptor type-5
- Dopamine 2 receptors
- GABA receptors
- L-type voltage-gated calcium channels
- Muscarinic acetylcholine receptors (mAChR)
- Neurotrophic Receptor Tyrosine Kinase 1 (NTRK1
- Nicotinergic acetylcholine receptor (nAChR
- Peroxisome proliferator activated receptor-γ(PPARs)
- Serotonin 5-HT6 receptor

DISBALANCE OF PHYSIOLOGICAL STATES OR PATHWAYS
- Oxidative stress
- Inflammation
- Calcium dyshomehostasis
- Metal dyshomehoastasis
- Mitochondial damage

Figure 1. Molecular targets for AD. Targets are classified into "established", if drugs directed toward these targets are available on the market, and "under investigation" if no drug toward these targets has already been approved. Based on the review article by Bjørklund *et al.* (2019) [2].

Since then, no new drug for AD has been approved by the health authorities, tacrine being withdrawn for hepatotoxicity reasons. Hence, the research in drug discovery for AD is still very active in the search of new

effective drug candidates: Figure 1 summarizes the main molecular targets under investigation in AD research [2].

Although a quite large number of molecular targets have been investigated in the search for new therapeutic avenues, the most intense research has been focused on amyloid and tau aggregation, on cholinesterase enzymes, on secretase enzymes implicated in the production of amyloid beta peptides (Aβ) and on kinases participating in the hyperphosphorylation of tau protein. The high number of investigations on these targets is partially due to the prominence of the cholinergic and amyloid hypotheses, followed by the tau hypothesis, which have led the drug discovery research in AD for decades, with alternative targets only emerging in more recent times.

This review will therefore discuss the main analytical techniques used to identify new chemical entities addressing AD in the last five years (January 2014-June 2019). The paper is divided into three parts, dealing with different analytical techniques: (a) spectroscopic methods; (b) MS-based methods; (c) microscopy-based methods. Major advantages and critical issues of these promising techniques are highlighted, and the methods of choice to obtain a complete view of the pathological mechanisms of AD, as well as new approaches, are discussed.

2. Spectroscopic methods

The most adopted assays for the screening of compounds designed and synthesized as inhibitors toward the most important targets of AD are based on spectroscopic measurements. Clear evidence of this aspect is the application of the ultraviolet-visible (UV-Vis)-based Ellman's assay for the screening of cholinesterase inhibitors [3] or the assays based on the use of fluorescent dyes such as thioflavin T (ThT) [4] for the selection of active compounds against the aggregation of Aβ or tau. Moreover, the importance of developing new and more efficient methods and the necessity to draw up alternative solutions to radiometric assays have led to the evolution of classical assays into new spectroscopic methods.

2.1 Fluorescence- and luminescence-based assays

Many assays based on the detection of fluorescence were developed adopting the fluorescence resonance energy transfer (FRET) principle, which is based on the energy transfer between a donor and an acceptor when they are in the resonance state. The efficiency of this phenomenon is strictly related to the distance between the donor and acceptor groups. FRET can be used in a wide range of applications, dealing with the detection of conformational changes for macromolecules or the investigation of ligands binding to their targets [5-9].

The use of FRET has been largely directed to the development of in-solution methods for the *in vitro* characterization of beta-secretase (beta-site amyloid precursor protein-cleaving enzyme 1 or BACE1) inhibitors. For this purpose, synthetic peptides, based on the sequence of the Swedish mutation of the amyloid precursor protein (APP) and bearing a fluorophore (donor group) and a quencher (acceptor group), were used as substrates [10]. In the non-cleaved substrate, the fluorescence of the donor is quenched by the adjacent acceptor, provided that the emission spectrum of the donor well overlaps to the absorption spectrum of the acceptor and that the two groups are positioned within the Förster radius of each other (which is about 3-6 nm and is defined as the distance at which half the excitation energy of the donor is transferred to the acceptor). When the peptide chain is cleaved by BACE1, the donor-specific fluorescence is no longer quenched and it can be measured [11].

The application of these substrates was not only circumscribed to in-solution methods: indeed, the same substrates were adopted for on-line methods based on the use of immobilized enzyme reactors (IMERs) containing BACE1 [12-14]. Recently, the FRET principle has been applied for the development of an inkjet printing-based assay for the screening of BACE1 inhibitor. A rhodamine-based substrate was printed on

parchment paper in order to be cleaved by the enzyme printed on the same spot. The inhibition was detected by monitoring the fluorescence profile obtained by maintaining the substrate concentration constant and by increasing the amount of inhibitor (Figure 2). One of the most important advantages of this method is the very low amount of enzyme and substrate required to carry out inhibition experiments. Indeed, this novel assay requires a 1.4×10^3 smaller quantity of BACE1 and substrate than the conventional in-solution assay with multi-well plate. The good reproducibility of results obtained for the evaluation of the inhibitory activity of well-known inhibitors makes this assay suitable for the HTS of BACE1 inhibitors [15].
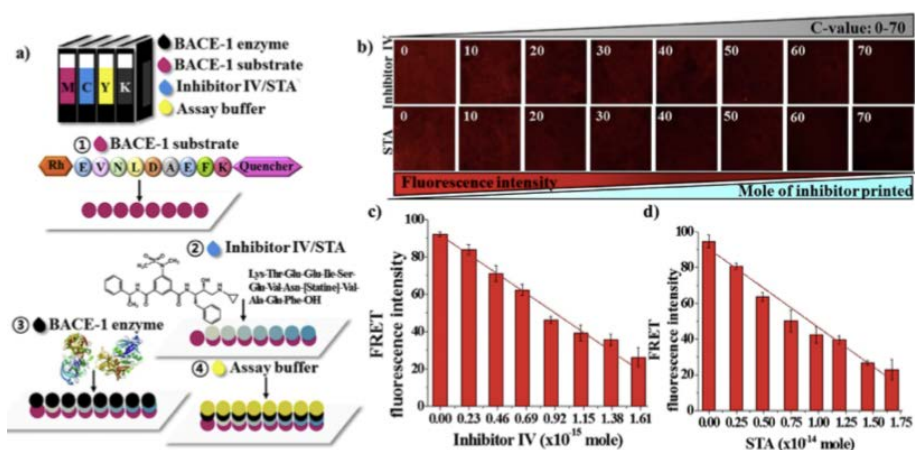
Figure 2. Detection of BACE1 inhibitory activities using inkjet printing. **(a)** Printing order of ink solutions to perform the inhibition assay. **(b)** Images of fluorescence produced after the cleavage of FRET peptide by BACE1 obtained with different amount of inhibitor printed. Quantitative plot of the reduction of fluorescence intensity obtained on the reaction spot for **(c)** Inhibitor IV and **(d)** peptide-based statine derivative STA. Fluorescence intensity was measured using a confocal microscope (λ_{exc} = 545 nm; λ_{em} = 585 nm). Reprinted from Ref. [15], Copyright (2018), with permission from Elsevier.

The same phenomenon can also be applied to detect protein–ligand binding. That was the case of protein kinase C (PKC), an enzyme correlated to cell signaling pathways and involved both in cancer and in AD. The crucial step of PKC activation is the binding of diacylglycerol (DAG) to the C1 domain [16]. The most common method used for the characterization of PKC ligands targeting to the C1 domain is a radioisotope assay [17-19]. A novel FRET-based competitive assay has been developed for the detection of PKC ligands. To this purpose, a DAG-lactone linked to diethylaminocoumarin at the *α*-alkylidene position (*sn*-2 DEAC-type DAG-lactone) and a fluorescein-labeled *δ*C1b domain (Fl-*δ*C1b) were synthesized as the donor and acceptor molecules, respectively. The donor shows moderate binding affinity for the *δ*C1b domain of PKC (residues 231 to 281), while the fluorescein moiety is bound to the Val[235] residue, at a suitable distance for the FRET

phenomenon to occur. When a test compound competes with the binding of the *sn*-2 DEAC-type DAG-lactone to the *δ*C1b domain of PKC, a decrease in the fluorescence intensity for fluorescein can be detected due to the displacement of the donor (Figure 3). The developed assay allows the screening of ligands for PKC but can be applied to the investigation of other protein–ligand interactions [20].
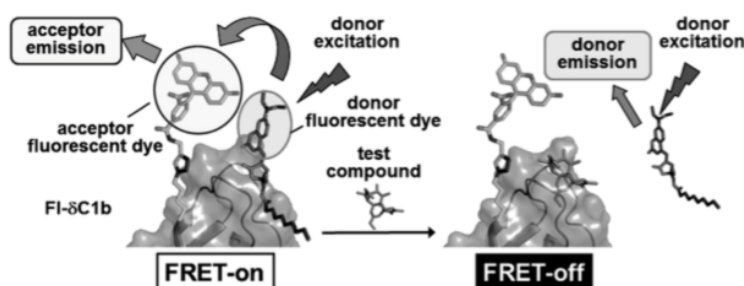
Figure 3. Schematic representation of the FRET-based competitive assay of PKC ligands. The FRET-on condition occurs in the presence of the donor (*sn*-2 DEAC-type DAG-lactone), which causes the fluorescent emission of fluorescein on the acceptor (Fl-*δ*C1b). A decrease in fluorescence intensity for the acceptor can be detected after displacement of the donor by a test compound (FRET-off). Reprinted with permission from Ref. [20].

Different studies were also performed applying fluorescently labeled peptides or targets for the characterization of target protein–ligand or protein–protein interactions. The application of a fluorescently labeled peptide allowed developing a peptide–tungsten disulfide (WS$_2$) nanosheet-based biosensing platform for the detection of BACE1 activity and inhibitors characterization (Figure 4). The sensing platform is obtained using the interaction between the peptide and the WS$_2$ nanosheet. In the absence of BACE1, the fluorescently labeled peptide is adsorbed onto the WS$_2$ nanosheet surface and fluorescence quenching occurs. In the presence of the enzyme, the hydrolysis of the peptide leads to the release of the fluorescent label. Since the fragment cannot be adsorbed on the WS$_2$ nanosheet, the fluorescence is restored. The monitored change in fluorescence is then related to the enzymatic activity. Different substrates can be used in this assay, since the WS$_2$ nanosheet can act as a common energy acceptor for different types of fluorescent dyes. Moreover, different proteases can be adopted as targets and studied by this simple and immediate method [21].
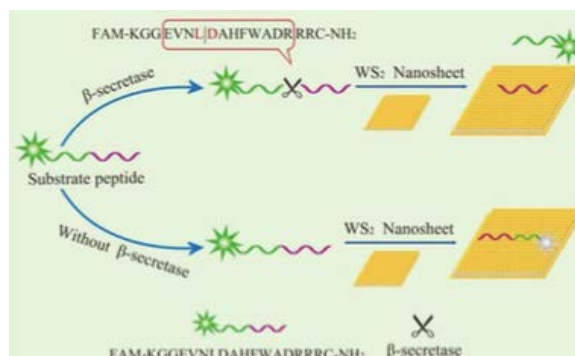
Figure 4. WS$_2$ nanosheet-based sensing platform for fluorescent analysis of BACE1. Republished with permission of Royal Society of Chemistry, from Ref. [21]. Copyright (2018); permission conveyed through Copyright Clearance Center, Inc.

Fluorescence-based assays can also be applied for the study of compounds able to interfere in some protein–protein interactions. That was the case of cellular prion protein (PrP^C) interacting with Aβ; PrP^C acts as a receptor for synaptotoxic oligomeric forms of Aβ in AD. Therefore, the identification of compounds able to bind to PrP^C and stabilize its native fold may be of considerable interest since these entities may act as pharmacological chaperones, blocking prion propagation and pathogenesis and inhibiting the binding of toxic species involved in AD. The development of HTS assays based on the use of a nitrobenzoxadiazole (NBD)-labeled protein allowed the screening of 1200 compounds and the selection of Chicago Sky Blue 6B as the first small PrP^C ligand capable of inhibiting Aβ binding. The fluorescence signal of the NBD label was monitored using 485 and 535 nm as excitation and emission wavelengths, respectively. Fluorescence intensities recorded after incubation of the PrP^C protein with different compounds and upon Aβ addition were compared to identify active compounds [22].

Other than new fluorescence-based assays, a novel luminescence turn-on assay has been recently developed for the detection of AChE activity. The assay, proposed by Law *et al.*, is based on the supramolecular self-assembly of alkynylplatinum(II) complexes. This assay is founded upon the self-assembly behavior of Pt(II) complexes through noncovalent Pt(II)···Pt(II) and π−π stacking interactions. In the presence of AChE, acetylthiocholine undergoes hydrolysis to thiocholine with the consequent *in situ* formation of a cationic Ag(I)–thiocholine coordination polymer. The aggregation is then facilitated by the electrostatic interactions between the anionic Pt(II) complex molecules and the cationic coordination polymer, leading to a low-energy red emission turn-on (Figure 5) [23].
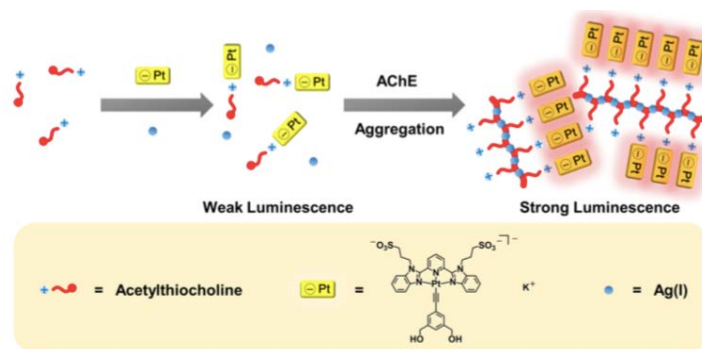
Figure 5. Rationale for the luminescence turn-on assay for AChE using anionic alkynylplatinum(II) complexes, acetylthiocholine and Ag(I) ions. Reprinted with permission from Ref. [23]. Copyright (2019) American Chemical Society.

2.2 Surface plasmon resonance (SPR) biosensing

The major targets involved in the etiology and development of AD, such as BACE1, glycogen synthase kinase 3β (GSK-3β) and AChE, were studied by biosensor–based approaches. In the last few decades, the application of biosensing devices has proven to be innovative and suitable for carrying out different kinds of analysis. Among the different types of optical biosensors, the SPR-based biosensor is considered a versatile and informative tool [24]. It is based on the detection of changes in refractive index occurring on the surface of a sensor chip as a result of the binding of biomolecules. A glass substrate and a thin gold film are the components that normally constitute the sensor surface. Indeed, the SPR phenomenon arises when light is reflected from a conducting film at the interface between two media of different refractive index (Figure 6) [25]. The binding of biomolecules to the sensor chip surface increases the refractive index of the solution near the sensor surface due to the changes in the momentum of the surface plasmons and their associated evanescent wave. The consequent change in the incident angle is related to an angle shift, which is directly proportional to the change in mass on the gold surface. Indeed, the response obtained is directly related to the mass of the analyte binding to the surface. Based on this principle, SPR biosensing can provide a qualitative evaluation on whether the molecules bind or not to the immobilized target and allows the quantitative determination of binding affinities and kinetic rate constants for the interaction. These features are relevant in the drug discovery process, since association (k_{on}) and dissociation (k_{off}) rate constants are important parameters for the characterization of a new hit compound [26].
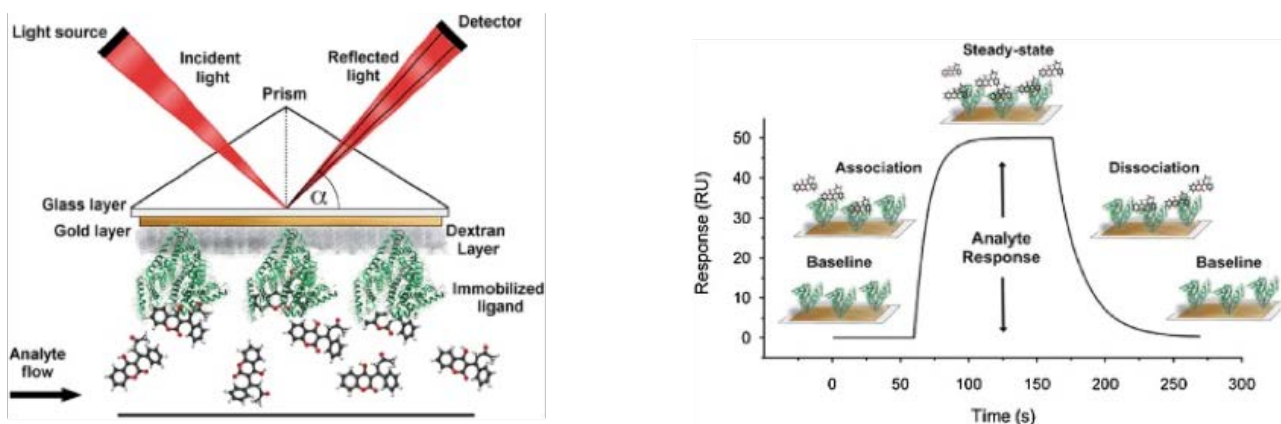
Figure 6. The SPR detection system and a typical sensorgram showing the association and dissociation steps occurring after ligand immobilization in a biosensor assay. Reprinted from Ref. [27], Copyright (2017), with permission from Elsevier.

From a practical point of view, the main advantage of this technique is that none of the interacting entities need to be labeled, which is convenient in terms of time and cost. Different immobilization strategies can be used, lowering the possibility of occluding binding sites and reducing the risk of false negative or positive signals. Moreover, the analyzed proteins are studied in a state as close to their native one as possible. On the other hand, target immobilization needs to be carefully chosen to avoid structural alterations, leading to a different behavior from the one observed in solution [28, 29]. Different strategies may be adopted for the immobilization of the ligand on the surface, such as covalent and capture coupling. Among the covalent coupling strategies, the most used is the amine coupling procedure. The high content of lysine residues in biomolecules makes amino groups usually available for linkage to the surface. In addition, both the biosensor and the biomolecules can be derivatized to introduce functional groups suitable for the coupling procedure on the biosensor surface or in the structure of the biomolecule. Indeed, the surface can be functionalized to have groups that can efficiently react with aldehydes or thiol groups [28].

A popular strategy to obtain a homogeneous population of oriented molecules on the surface is the affinity-capture approach, which exploits antibody-antigen interactions, streptavidin-functionalized surfaces for biotinylated ligands or metal chelation for histidine-tagged ligands [28]. Due to the wide range of protocols that can be adopted for the immobilization of a ligand on the surface, the choice of the strategy is closely related to the chemical properties of the biomolecules and its stability. In most cases, the application of SPR biosensing is specifically directed at evaluating the affinity of active molecules toward a selected target, which is usually expressed in terms of the equilibrium dissociation constant (K_D) of the binding complex. The experimental procedure followed to reach the K_D value of molecules toward the immobilized target consists in

carrying out the immobilization protocol for two flow cells: a reference cell is generated by activation and deactivation without any target protein, while the sample cell containing the enzyme is generated through activation, immobilization and deactivation steps. The tested molecules solutions are flushed on the chip surface. The obtained sensorgrams are then subjected to the automatic correction for non-specific bulk refractive index effect. The blank-corrected sensorgrams are used to derive the affinity constants by curve fitting using an appropriate kinetic model.

In the drug discovery process, SPR biosensing can be fruitfully exploited to perform structure-affinity relationship (SAR) studies for the optimization of hit scaffolds into more active and clinically useful lead drugs. Han *et al.* applied a SPR-based approach to the evaluation of a class of pyrazole-5-carboxamides as potential inhibitors of the receptor for advanced glycation end-products (RAGE) [30]. RAGE–Aβ interactions promote the transport of Aβ into the brain and are suggested to activate the nuclear factor kappa-light-chain-enhancer of activated B cells (NF-κB), a transcription factor involved in many inflammatory responses. A NF-κB-responsive element in the RAGE gene promoter then induces the hyperexpression of RAGE [31, 32] and an increase in Aβ accumulation and inflammation, in a positive feedback loop leading to a worsening in AD condition. The inhibition of RAGE is therefore considered a promising strategy for decreasing the rate of deposition of Aβ and inhibiting the inflammatory response of Aβ in the brain. All the synthesized pyrazole-5-carboxamides derivatives were biologically evaluated and ranked by a SPR-based assay for their affinity to the immobilized receptor using biotinylated RAGE. The consequent SAR allowed the identification of the most active compound, and the binding interaction was confirmed by docking simulations [30].

The capturing strategy of $Aβ_{1-42}$ and tau in flow cells was used to characterize the most promising compound belonging to the class of acridone derivatives designed and synthesized by Lv *et al.* [33]. The compounds were tested as inhibitors of both Aβ and tau aggregation. The adopted experimental conditions are reported in Table 1. The blank-corrected sensorgrams were analyzed using the Langmuir model to fit the kinetic data. The non-covalent inhibition for the most promising 1,2,3,4-tetrahydro-1-acridone was assessed by SPR analysis giving rise to the possibility of further development for this molecule [33].

Table 1. Experimental conditions adopted for the reported studied based on the SPR methodology.

Ligand(s)	Sensor Chip	Immobilization Strategy	Immobilization Buffer	Running Buffer	Immobilization Level (RU)	Ref.
RAGE [1 µg/mL]	NLC (Bio-Rad)	biotinylation	–	TBS-T + 2% v/v DMSO 100 µL/min	–	[30, 34]

Ligand(s)	Sensor Chip	Immobilization Strategy	Immobilization Buffer	Running Buffer	Immobilization Level (RU)	Ref.
BACE1 [20 µg/mL] 10 mM acetic acid pH 4.5	CM5 (Biacore)	amine coupling	–	PBS pH 7.4 + 5% v/v DMSO 30 µL/min	7500–8000	[35]
ABAD [10 µg/mL] PBS pH 5.0	CM5 (Biacore)	amine coupling	PBS-T pH 7.4	PBS-T pH 7.4	–	[36]
GLP-1R	-	amine coupling	PBS pH 7.4	PBS pH 7.4 + 0.1% v/v DMSO 20 µL/min	–	[37]
anti-Aβ antibody 4G8	GLC (Bio-Rad)	amine coupling	–		5000	[38]
Aβ [10 µM] 10 mM sodium acetate pH 3	CM5 (Biacore)	amine coupling	–	HBS-T pH 7.4 10 µL/min	–	[39]
Tau/Aβ [100 µg/mL] 20 mM PBS pH 7.4 + 0.005% v/v Tween-20	GLH (Bio-Rad)	capturing	–	–	–	[33]
CypD [20 µg/mL] 10 mM sodium acetate pH 5.5	CM5 (Biacore)	amine coupling	–	HBS-T pH 7.4 + 2% v/v DMSO 20 µL/min	–	[40]
AChE 0.1 M PB pH 5.0 + 0.33% v/v Triton X-100	CM5 (Biacore)	amine coupling	HBS	PB-T pH 8.0 75 µL/min	7000	[41]

HBS: 10 mM HEPES + 150 mM NaCl + 3 mM EDTA; HBS-T: HBS + 0.005% v/v Tween 20; PBS-T: 10 mM PB + 150 mM NaCl + 0.005% v/v Tween 20; PB-T: 100 mM PB + 0.025 v/v Tween 20; TBS-T: 20 mM Tris + 150 mM NaCl + 0.1% v/v Tween 20.

The SPR methodology was also applied for the characterization of a series of 2-substituted-thio-*N*-(4-substituted-thiazol/1*H*-imidazol-2-yl)acetamide derivatives as BACE1 inhibitors [35]. BACE1 was immobilized adopting the conditions described in Table 1. The blank-corrected sensorgrams were then used to derive the affinity constants by curve fitting using a steady-state model.

Valaasani *et al.* employed SPR biosensing to study two benzothiazole phosphonate derivatives as inhibitors of the mitochondrial Aβ binding alcohol dehydrogenase (ABAD), a promoter of (Aβ)-mediated mitochondrial and neuronal dysfunction with consequent decline in transgenic AD mouse models [36]. The protein was covalently immobilized on a CM5 sensor chip using a standard amine coupling reaction (Table 1). The kinetic analysis of ligand binding was carried out by fitting data to the Langmuir 1:1 binding model:

$$R_{eq} = R_{max} \cdot \frac{c}{c + K_D},$$ (1)

where c (M) is the inhibitor concentration, R_{eq} (RU) is the response at the steady state and R_{max} (RU) is the maximal response. Both tested compounds showed strong binding affinities to ABAD (K_D values in the nanomolar range), in agreement with their biological activity since they are able to reduce ABAD enzymatic

binding activity, reduce the calcium-induced formation of the mitochondrial permeability transition pore (mPTP), decrease the Aβ mitochondrial dysfunction and to increase cytochrome c oxidase and adenosine triphosphate (ATP) [36].

Another interesting application concerned compound P7C3 as a potent neurogenesis-promoting agent able to bind to the glucagon-like peptide 1 receptor (GLP-1R), which is involved in regulating the expression of neurogenesis-related proteins [37]. The mechanism of action of P7C3 was studied and appeared to be unique compared to that of other active derivatives of the same class. The binding of P7C3 to GLP-1R protein was analyzed by SPR biosensing after immobilization of the receptor on an amine coupling sensor chip (Table 1). The experimental K_D value was derived applying a 1:1 binding model, and the results were in agreement with molecular modeling predictions [37].

The SPR assay was also adopted for other purposes, such as the detection of the high-affinity interaction (K_D = 1 nM) of the chaperone clusterin with biologically relevant Aβ$_{1-42}$ oligomers [38]. Several classes of molecules (peptides, antibodies, proteins and molecular chaperones) influence the aggregation of Aβ peptides [42-45]. Molecular chaperones are endogenous proteins whose role is to suppress the formation of aggregates and promote the clearance of misfolded species [42, 43]; among them, clusterin (apolipoprotein J) is a chaperone whose gene locus is the third strongest known genetic risk factor for late-onset AD [46]. The sensing surface was prepared by immunoaffinity capture using immobilized anti-Aβ antibody 4G8; the investigation of the specific binding of clusterin for a subpopulation of Aβ$_{1-42}$ oligomers was then carried out. These oligomeric species were demonstrated to be biologically active *in vivo* [47]. The results showed that a sub-stoichiometric concentration of clusterin prevented oligomers to interact with the antibody 4G8. This indicates that the chaperone protects some hydrophobic residues exposed on the oligomeric assemblies. Since the exposure of hydrophobic motifs is considered fundamental for the toxicity of oligomers [48], it was possible to speculate the selectivity of clusterin toward these toxic oligomers.

SPR was also used to investigate interaction between Aβ$_{1-42}$ and glycogen synthase kinase 3α (GSK-3α). The tau hyperphosphorylation mediated by GSK-3α was found to be stimulated by Aβ$_{1-42}$ in an *in vitro* phosphorylation assay [39]. The SPR study based on a sensing surface containing Aβ$_{1-42}$ allowed characterizing the interaction in terms of K_D. The immobilization was carried out using Aβ$_{1-42}$ as monomer. After coupling on the dextran matrix (Table 1), the peptide most likely exists as a mixture of oligomeric and monomeric species. Hence, the high affinity parameter refers to the binding of GSK-3α to both monomers or

oligomers [39]. This finding also represents an opportunity to study the early molecular events in the disease, to provide a deeper understanding of kinase activation and to find factors able in modulating the affinity.

Park *et al.* used SPR to study cyclophilin D (CypD), a protein implicated in the formation of mPTP, which leads to the disruption of mitochondrial homeostasis with consequent cell death. Moreover, since the formation of mPTP promoted by CypD in brain mitochondria occurs upon the binding to Aβ, CypD is considered a promising AD target. The aim of the study was to assess whether a pool of compounds, previously selected by a combination of virtual screening and cell-based assays, could directly bind CypD. After CypD covalent immobilization on CM5 sensor chip by amine coupling a K_D value in the nanomolar range was found for one of the tested compounds. These results were consistent with the predicted binding mode [40].

The use of a SPR-based approach has also been proposed as a complement to the most frequently used methods for the screening of AChE inhibitors, namely those based on the electrochemical detection of choline and acetylcholine using IMERs [49, 50], chemiluminescence-based methods [51, 52] or Ellman's spectrophotometric method [3]. The first application of an AChE sensing surface (based on AChE from *Electrophorus electricus*) for the characterization of inhibitors was reported by Milkani *et al.* in 2011 which used the functionalized surface to study two AChE inhibitors, i.e. neostigmine and eserine [53]. Recently, a SPR-based assay was developed using the human form of the enzyme by Fabini *et al.* [41]. The sensing surface was obtained by amine coupling (Table 1). The same protocol, apart from the enzyme immobilization was adopted for the reference channel.

The studied inhibitors were tacrine and donepezil (mixed-mode competitors), galantamine and edrophonium (substrate-competitive). Solutions of different compounds were presented on the functionalized surface in order to evaluate the capability of discriminating different inhibitors. The results obtained in terms of affinities were consistent with the inhibitory potencies reported in literature. The analysis revealed rapid on/off rates for the complexes formed by AChE with tacrine and edrophonium, as evinced from the squared-shaped sensorgrams (Figure 7). On the other hand, slower dissociation events were observed for galantamine–AChE and donepezil–AChE complexes. The application of the 1:1 binding model (Eq. 1) allowed obtaining the association and dissociation rate constants for each compound.
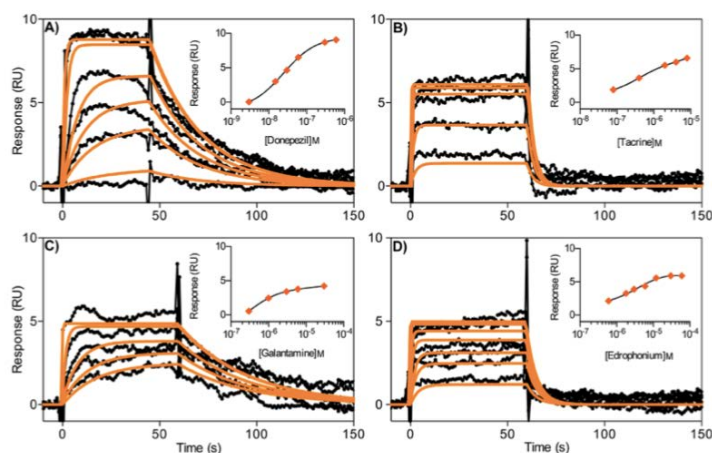
Figure 7. Affinity and kinetic studies of the four selected inhibitors binding to the immobilized human AChE chip surface: donepezil **(A)**, tacrine **(B)**, galantamine **(C)**, edrophonium **(D)**. Reprinted from Ref. [41], Copyright (2018), with permission from Elsevier.

Compounds with similar K_D values may show large differences in both k_{on} and k_{off} values, resulting in different *in vivo* efficacy. The determination of rate constants can help finding a good balance between therapeutic and adverse effects by correlating the duration of action of a drug to the kinetic properties of its binding interaction with the target. Residence times were then derived from the dissociation rate constants, and compounds were classified in two groups: tacrine and edrophonium, showing a residence time lower than 5 s, were classified as fast-reversible binders, while galantamine and donepezil were characterized as slow-reversible binders. All compounds show a quite fast dissociation from their binding site; this behavior might be explained by the nature of the target enzyme. AChE is a terminator of signal transduction and some adverse effects can arise when the inhibitory effects are extensively prolonged [54, 55].

Since the pharmacological effects of drugs are influenced by their ADMET profiles, the authors also explored the binding of AChE inhibitors to human serum albumin (HSA); the measured affinities were then converted to bound fractions. A nice correlation with the pharmacokinetic data obtained in clinical study was observed for donepezil and galantamine [56], and the high percentage of binding for donepezil suits well with its duration of action. The SPR application reported by Fabini *et al.* may be proposed as a solution to implement classic inhibition data with a detailed characterization of the pharmacokinetic profile of new drug candidates.

2.3 Circular dichroism (CD) spectroscopy

Circular dichroism (CD) is a physical phenomenon responsible for the different absorption of left and right circularly polarized radiation by chiral molecules. The spectroscopic evaluation of CD across the UV (electronic

CD or ECD) and IR (vibrational CD or VCD) spectral regions can provide useful information about the stereochemical properties of a chemical system, such as the absolute configuration of small molecules and the conformational arrangement of biological macromolecules or supramolecular assemblies at equilibrium [57-59].

CD spectroscopy in the far-UV region (260–190 nm) is routinely employed to determine the secondary structure of proteins in solution [60], since the different secondary structures display distinctive CD signatures: for instance, disordered proteins are characterized by a negative CD peak centered at around 200 nm with a broad negative shoulder at longer wavelengths, while β-strands show a negative CD peak with maximum intensity at 215 nm followed by a positive peak below 200 nm [61]. The effect of ligand binding on the secondary structure of several targets involved in AD has been investigated in recent years, including AChE [62, 63], APP [64] and the islet amyloid polypeptide (IAPP) [65].

One of the key molecular mechanisms involved in AD is the misfolding of amyloidogenic proteins, such as Aβ and tau, from a prevalently disordered conformation to a secondary structure rich in β-strands [66]; this conformational transition is considered as the triggering event of amyloid oligomerization and aggregation into senile plaques. It is thus not surprising that the main application of CD spectroscopy in the field of AD drug discovery is focused on the evaluation of potential inhibitors of amyloid aggregation as modulators of misfolding phenomena (Table 2).

Table 2. CD studies on amyloid misfolding in AD drug discovery research (January 2014–June 2019).

Target	Ligand(s)	CD assay	Ref.
Aβ$_{1-42}$	J2326	50 µM target + 10 µM ligand 6(+1) h incubation	[67]
	chitosan oligosaccharides	50 µM target + 2.5–5 mg/mL ligand 48 h incubation	[68]
	poly(LVFF-*co-β*-amino ester)	20 µM target + 40–120 µM ligand no incubation, s.s.e. (Jasco PSSE)	[69]
	meso-tetra(4-sulfonatophenyl)porphyrin	40 µM target + 0.05–10 µM ligand 24 h incubation (dark/light, aerobic/anaerobic)	[70]
	tacrine and bis(heptyl)-cognitin	20 µM target + 1–10 µM ligand 48 h kinetics	[71]
	Aβ$_{39-42}$, (−)-epigallocatechin-3-gallate and CLR01	50 µM target + 250 µM ligand 4 h kinetics	[72]
	(*R*)-α-trifluoromethylalanine-containing tetrapeptide	50 µM target + 500 µM ligand 96 h kinetics, s.s.e. (CDfriend)	[73]
	hydralazine	22 µM target + 10 µM ligand 48 h incubation, s.s.e. (CDPro)	[74]
	NPT-440-1	44 µM target + 4.4 µM ligand 15 min incubation	[75]
	hematoxylin	25 µM target + 25 µM ligand 24 h kinetics, s.s.e. (BeStSel)	[76]

Target	Ligand(s)	CD assay	Ref.
	5,10,15,20-tetrakis(*N*-methyl-4-pyridyl)porphyrin	25 µM target + 25 µM ligand 3(+2) h incubation	[77]
	triazine-triazolopyrimidine hybrids	20 µM target + 20 µM ligand 24 h kinetics	[78]
	amyloid inhibitory peptoids	20 µM target + 20–200 µM ligand 24 h incubation	[79]
	3-morpholinosydnonimine hydrochloride	25 µM target + 25–125 µM ligand 20 h kinetics	[80]
	oligopyridylamide α-helical mimetics	15–20 µM target + 15–20 µM ligand 24 h incubation	[81, 82]
	oligomeric polypeptides	20 µM target + 20 µM ligand 72 h incubation	[83]
	oligoquinoline derivatives	20 µM target + 20 µM ligand 48 h kinetics	[84]
	triterpenoids	25 µM target + 50 µM ligand 24 h kinetics	[85]
	1,2,3,4-tetrahydro-1-acridone analogues	50 µM target + 20 µM ligand 24 h kinetics	[33]
	chalcone derivatives	50 µM target + 50 µM ligand 40 d kinetics	[86]
	deuterohemin-peptide conjugate DhHP6	75 µM target + 25 µM ligand 72 h incubation, s.s.e. (Jasco PSSE)	[87]
	CORM-3	50 µM target + 50–250 µM ligand 52 h kinetics	[88]
	3-bis(pyridin-2-ylmethyl)aminomethyl-5-hydroxybenzyltriphenylphosphonium bromide	40 µM target + 80 µM ligand 24 h incubation	[89]
$A\beta_{1-40}$	1,4,7-triazacyclononane and bis(2-pyridylmethyl)amine	50 µM target + 200 µM ligand 4 h incubation	[90]
	dipentaerythritol glucoclusters	30 µM target + 6–150 µM ligand 72 h incubation, s.s.e. (CONTIN)	[91]
	water-soluble Zn-containing phthalocyanines	100 µM target + 2 µM ligand 2 h incubation, s.s.e. (Jasco PSSE)	[92]
	quinolizidinyl derivatives	50 µM target + 25 µM ligand 7 h kinetics	[93]
	polyethylenimine–perphenazine conjugates	50 µM target + 65 µM ligand 45 h kinetics	[94]
	N^1-(7-nitrobenzo[c][1,2,5]oxadiazol-4-yl)-N^2,N^2-bis(pyridin-2-ylmethyl)ethane-1,2-diamine	50 µM target + 200 µM ligand 4 h incubation	[95]
tau	crocin	20 µM target + 100 µg/mL ligand 120 h incubation	[96]
AcPHF6	cyclic D,L-*α*-peptides	20 µM target + 10 µM ligand no incubation	[97]
	5-arylidene-2,4-thiazolidinedione derivatives	100 µM target + 20 µM ligand 2 h incubation	[98]

In recent years, CD assays on misfolding have been primarily applied to the characterization of $A\beta_{1-42}$ [33, 67-89] and $A\beta_{1-40}$ [90-95] aggregation; the misfolding of tau has also been investigated by CD spectroscopy using either the full protein [96] or the hexapeptide AcPHF6, derived from a sequence in the third repeat domain of tau (residues 306–311) [97, 98].

CD studies on misfolding are usually performed by incubating the protein in the absence and in the presence of ligands at single or multiple concentrations. The effect of ligand binding on misfolding can then be determined at a single time after the conformational transition of the isolated protein has taken place, or its evolution can be evaluated at different times after sample preparation (Figure 8). After CD analysis, the relative contribution of disordered and β-strand structures can be derived using one of the available algorithms for secondary structure estimations (s.s.e.), such as CONTIN [91] or BeStSel [76]; alternatively, the conformational transition can be described by the evolution of the CD signal at a single wavelength (usually at the maximum of the negative CD peak for β-strands) as a function of time [93] or concentration of ligand [65].
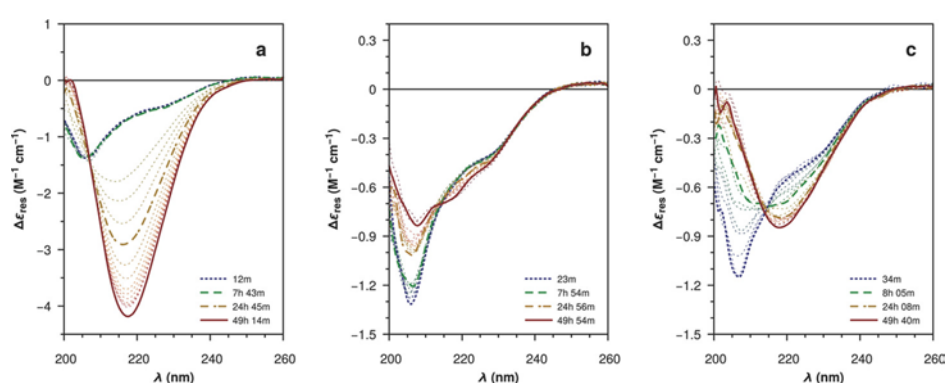
Figure 8. CD spectra of Aβ$_{1-42}$ samples at different times after sample preparation: **(a)** in the absence of CORM-3; **(b)** in the presence of CORM-3 at 1:1 molar ratio; **(c)** in the presence of excess CORM-3 at 5:1 molar ratio. Reprinted from Ref. [88]. Copyright (2019) American Chemical Society.

The experimental conditions used for the incubation step (target and ligand concentrations, buffer composition, pH, temperature, presence of aggregation-inducing co-factors) have a huge and defining impact on the kinetics of amyloid misfolding. Unfortunately, a wide variety of incubation conditions have been reported in the literature: CD studies on Aβ$_{1-42}$ were carried out with protein concentrations ranging from 15 μM [81] to 75 μM [87] and incubation times ranging from 15 minutes [75] to 40 days [86]. The lack of a widely recognized and standardized protocol to perform CD assays on Aβ and tau leads to the low degree of reproducibility observed across studies: for instance, the precipitation of insoluble aggregates is a common but frequently overlooked issue that gives rise to strong light scattering artifacts and greatly affects the quality of CD spectra.

These limitations might help understanding why CD assays are not employed as routinely as other well established biophysical and analytical approaches to amyloid aggregation studies. Nevertheless, CD spectroscopy is the technique of choice to follow the earliest stages of Aβ and tau aggregation, because it enables the observation of monomers evolving into soluble oligomers while the proteins are still in solution. In

this framework, the combination of CD studies with ThT-based fluorescence assays and microscopy-based methods represents a valuable and comprehensive strategy to investigate the inhibitory activity of potential drugs at all the different stages of amyloid aggregation.

2.4 Nuclear magnetic resonance (NMR) spectroscopy

Nuclear magnetic resonance (NMR) arises from the absorption of radiofrequency radiation by atomic nuclei subjected to a strong external magnetic field; the resonance frequencies of the resulting transitions between nuclear spin states are strongly influenced by the chemical environment surrounding the nuclei [99]. NMR spectroscopy is a powerful technique that allows to gather extremely detailed information about molecular structures with resolution at the atomic level, and the development of several multi-dimensional experiments with complex pulse sequences opened the path for the application of NMR spectroscopy to proteins and protein–ligand complexes [100-102]. For instance, two-dimensional heteronuclear single quantum coherence (2D HSQC) experiments can be used to gain insight on the secondary structure of proteins, thanks to the correlation of signals arising from the amide N-H groups in the protein backbone, also allowing the assignment of peaks to single amino acidic residues [103]. A recent application of ^1H–^{13}C and ^1H–^{15}N HSQC NMR to study $A\beta_{1-40}$ highlighted the ability of chlorin e6, a porphyrin photosensitizer, to interact with the *N*-terminal region and selectively react with histidine residues, reducing the binding affinity of $A\beta_{1-40}$ toward Cu^{2+} and inhibiting amyloid aggregation [104]; ^1H–^{15}N HSQC studies were also employed to evaluate the inhibitory effect of oligopyridylamine- and oligoquinoline-based foldamers on the misfolding of $A\beta_{1-42}$ [81, 82, 84].

Protein-based NMR binding assays rely on the perturbation of chemical shifts observed for residues involved in the interaction with ligands. The improvement in analysis time introduced by ^1H–^{15}N band-selective optimized-flip-angle short-transient heteronuclear multiple quantum coherence (SOFAST-HMQC) [105] experiments has enabled robust and reliable evaluations of such perturbations on uniformly ^{15}N-labeled proteins. In the field of AD drug discovery, ^1H–^{15}N SOFAST-HMQC experiments have been primarily employed to investigate the interaction of $A\beta_{1-40}$ and $A\beta_{1-42}$ with several potential inhibitors of amyloid aggregation, such as glycosylated polyphenols [106], anthoxanthins (Figure 9) [107, 108], triterpenoids [85], multifunctional aminoquinoline compounds [109, 110], quinoline-triazole derivatives [111], and peptides [112], as well as tramiprosate [113] and (*R*)-apomorphine [114]; in all these inhibition studies, the concentration of Aβ was kept at 80 μM or lower, with sample volumes usually below 600 μL. Another popular protein-based NMR experiment, transverse relaxation-optimized spectroscopy (TROSY) [115], has been recently applied to study

the interaction of Aβ₁₋₄₂ with a clioquinol-moracin M hybrid, developed as a multitarget-directed ligand (MTDL) with metal chelating properties and inhibitory activity toward phosphodiesterase 4D (PDE4D) [116].
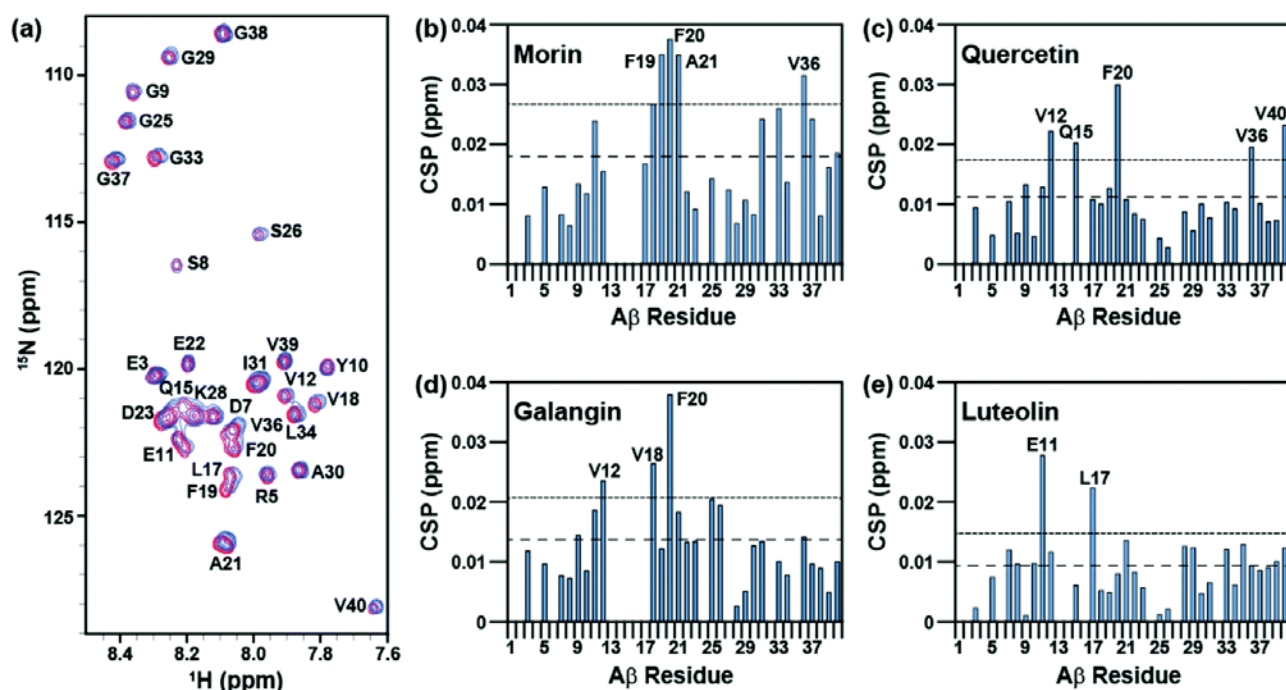
Figure 9. ^1H–^{15}N SOFAST-HMQC NMR analysis of Aβ–flavonoid interactions. **(a)** Spectra of ^{15}N-labeled Aβ₁₋₄₀ in the absence (red) and in the presence of a 10:1 molar excess of morin (blue). **(b–e)** Chemical shift perturbations (CSP) on ^{15}N-labeled Aβ₁₋₄₀ upon the addition of morin, quercetin, galangin and luteolin. Average CSP values (dashed) and standard deviations (dotted) were plotted for reference: higher values are indicative of noticeable interactions of flavonoids with the corresponding residues. Reproduced from Ref. [108] – published by The Royal Society of Chemistry.

On the other hand, saturation transfer difference (STD) experiment is one of the most popular approaches for ligand-based NMR binding assays [117]. STD NMR exploits the negative nuclear Overhauser effect (NOE) acting on bound ligands when the protein is selectively irradiated, allowing to confirm binding events and determine the so-called group epitopes of ligands, i.e. the atoms involved in the interaction. In the field of AD drug discovery, this powerful technique has been fruitfully applied to investigate the binding of known and potential cholinesterase inhibitors, such as galantamine [118], donepezil and donepezil-based hybrids [119, 120], (S)-rivastigmine [121], gallic acid, scopoletin and 4-methylumbelliferone [122], as well as isoquinolone [118], 3-hydroxyoxindole [123] and coumarin derivatives [124]; in some of these studies, transferred NOE spectroscopy (Tr-NOESY) [125] experiments were used in combination with STD NMR to gain insight on the bound conformation of ligands [120, 122, 124]. STD NMR has also been employed to study the interaction of Aβ₁₋₄₂ with flavonoids [126, 127], identify dicaffeoylquinic acids as potential inhibitors of amyloid aggregation

in a complex mixture of natural compounds extracted from the roots of imperatoria (*Peucedanum ostruthium*) [128], and investigate the modulation of Aβ–transthyretin interactions by iodoflunisal and (−)-epigallocatechin gallate [129].

Outside the realm of multi-dimensional NMR, a noteworthy application of ^{1}H NMR spectroscopy to AD drug discovery is concerned with the inhibition of the enzymatic activity of AChE: to this purpose, a kinetic assay was developed exploiting the different chemical shifts for the methyl groups of acetylcholine (2.24 ppm) and acetate (2.16 ppm) [130]. This approach was recently employed to determine the inhibition of AChE from *Electrophorus electricus* by guanylhydrazones [131, 132], some tacrine analogues [133] and semicarbazone derivatives [134].

## 2.5 Fourier-transform infrared (FT-IR) spectroscopy

Although infrared (IR) spectroscopy is mostly used in AD for diagnostic purposes, the application of Fourier-transform (FT)-IR spectroscopy for the structural characterization of proteins has largely increased. Some FT-IR based assays have been carried out for investigating more deeply the mechanism of action of some anti-aggregating molecules. The analysis is based on the detection of amide bonds, which display distinct IR signals depending on the different folding of proteins and peptides. The amide I (1600–1690 cm^{-1} C=O stretching) and amide II (1480–1575 cm^{-1} CN stretching, NH bending) are the two most prominent vibrational IR bands used to reveal conformational changes in the backbone of peptides and proteins [135]. On this basis, the conformational change of Aβ$_{25–35}$ due to aggregation and the subsequent restoration upon treatment with natural extracts was evaluated [136, 137]. The transition from unordered to β-sheet structure was related to an increase in absorption at 1628 cm^{-1}. A maximum absorbance at 1518 cm^{-1} was detected for the Aβ$_{25–35}$ aggregates, whereas for the treated peptide a shift in the maximum absorbance at 1550 cm^{-1} was detected. The results obtained by FT-IR analysis demonstrated the ability of the extract from *Gelidiella acerosa* to interact with Aβ$_{25–35}$ and prevent its aggregation [137].

2.6 UV resonance Raman (UV-RR) spectroscopy

UV resonance Raman (UV-RR) spectroscopy has been employed to follow the change in the secondary structure of tau during its side-chain packing and fibril formation, in the presence of heparin as inducer. The tau fibrillization process is characterized by two stages: the first one involves the formation of nonfibrillar, dye-negative "pre-tangles", while the second stage is related with the formation of mature, dye-positive

neurofibrillary tangles [138]. ThT fluorescence assays, light scattering-based methods and electron microscopy studies are useful in detecting ligand-induced, nucleation-dependent polymerization, but cannot distinguish between the different stages of conformational conversion and fibril growth. Conversely, UV-RR spectroscopy allows monitoring the formation of fibrils in both stages, since the position and the intensities of the amide Raman bands varies in two different steps, corresponding to the stages of the fibril formation process.

Spectral changes for the Am III$_3$ (the most sensitive frequency of the Am III region) and Am I amide bands give the opportunity of monitoring the aggregation process. For instance, Am III$_3$ bands in the 1240−1279 cm^{-1} region can be assigned to disordered structures, while bands in the 1220−1230 cm^{-1} region can be ascribed to β-sheets. Hence, the change in band position from 1238 cm^{-1} to 1230 cm^{-1} is typically observed upon transition from unordered to β-sheet structures. For the Am I band, a change from 1681 cm^{-1} (monomer in the absence of heparin) to 1670 cm^{-1} (aggregated fibrillar process) occurs during tau fibril formation (Figure 10). That is important for understanding the structural events that occur during the aggregation of tau and give the opportunity of designing and selecting new and specific aggregation inhibitors [139].
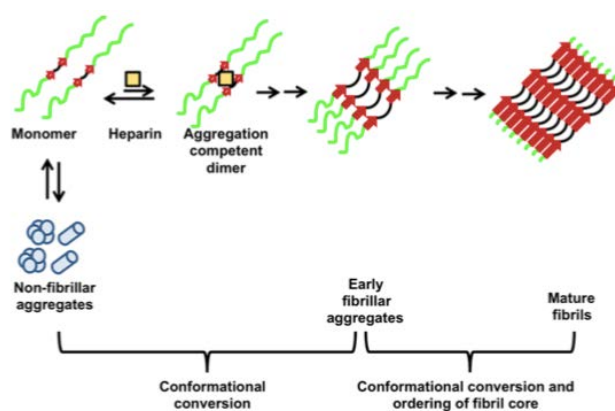
Figure 10. Schematic working model for the formation of fibrils by the repeat domain of tau in the presence of heparin. Reprinted with permission from Ref. [139]. Copyright (2014) American Chemical Society.

2.7 Fluorescence correlation spectroscopy (FCS)

Fluorescence correlation spectroscopy (FCS) is a correlation analysis of fluctuations in the intensity of fluorescence; this technique enables the detection of molecular motion at the nanomolar level in small sample volumes, thus allowing real-time monitoring of protein–protein interactions. FCS can be successfully used to monitor protein aggregation in real time using a mixture of labeled (in trace amount) and unlabeled (in large excess) proteins or peptides. Since the unlabeled molecule is in large excess, the fluorescent species remain

constant, while the diffusion time gradually decreases. Fluctuations in fluorescence reflect variations of the diffusion properties of the species in solution, which depend on the size of the species in solution and on changes in the ratio between free and labeled molecules in the forming aggregates. The technique allows examining whether a candidate inhibitor can interfere with protein aggregation, as well as investigating inhibition mechanism. This approach has been applied to the study of the anti-aggregating properties of a natural compound from *Centella asiatica* [140] and a peptidomimetic derivative [141] toward $A\beta_{1-42}$.

3. Mass spectrometry (MS)-based methods

Since the development of electrospray ionization (ESI) and other soft ionization techniques, as matrix-assisted laser desorption ionization (MALDI), MS has been fruitfully employed for a large and steadily increasing range of applications [142]. Recently, MS has been defined as a "multifaceted weapon" exploitable in the battle against AD [143]. MS, indeed, has been widely employed to unveil the molecular mechanisms at the basis of AD, assess new biomarkers and screen the efficacy of new potential drugs [143]. In the attempt to develop new multipotent drugs against AD, MS has been predominantly used to screen anti-Aβ agents, characterize the target protein–ligand interactions, identify promising active molecules through fishing experiments and assess target enzyme activity by monitoring the product formation. In the following subsections, the main MS-based analytical approaches in the context of AD drug discovery, along with the most significant examples, are reported and critically discussed.

3.1 Assessment of anti-Aβ agents

The amyloid hypothesis proposes that the accumulation of Aβ leads to synaptic dysfunction, neurodegeneration, and ultimately AD symptoms; therefore, the vast majority of potential disease-modifying treatments developed in recent years has been directed against Aβ and includes molecules capable to inhibit secretase enzymes or Aβ aggregation [144, 145]. Secretase inhibition, however, is problematic since these enzymes can cleave APP and other substrates involved in different biological processes [146]. Among the inhibitors of Aβ aggregation, several organic molecules, peptides or peptidomimetics and nanoparticles have been recently developed and their activity has been often assessed exploiting MS-based analytical tools [147].

The ability to screen for compounds able to disrupt protein aggregation is one of the ultimate in the field of AD drug discovery; therefore, diverse analytical approaches have been exploited to assess the inhibition of fibril formation, including microscopic and spectroscopic techniques along with immunology-based methods for quantification of Aβ [148]. However, the assessment of the potentially toxic oligomers destined to amyloid fibril formation is a significant challenge because of the heterogeneous, transient and low-populated nature of these species. The most mentioned biophysical techniques lack the sensitivity and the resolution for their detection and characterization. In the past, MS-based analytical approaches have shown to be extremely fruitful both for the assessment of the kinetic of aggregation of Aβ peptides and for the development of anti-Aβ agents [149-151].

Recently, a great contribution to the fine characterization of Aβ soluble oligomers and to the assessment of the early-stage mechanism of Aβ aggregation has been offered by the combination of ion mobility and mass spectrometry (IM–MS) [142, 152-154]. Using an ion mobility–mass spectrometer, Aβ soluble forms are separated not only based on their *m/z* value, but also on their mobility through a buffer gas on a millisecond timescale. Depending on the time necessary to pass through the buffer gas in the ion mobility spectrometer, different Aβ oligomers are characterized by different arrival time distributions (ATD) (Figure 11).
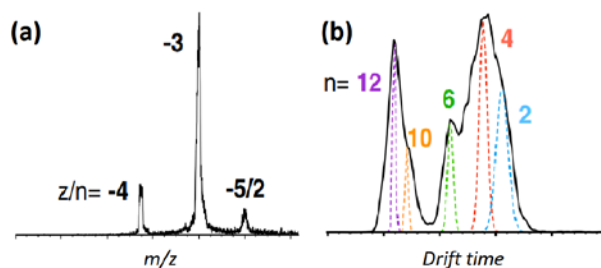

Figure 11. $Aβ_{1-42}$ mass spectrum **(a)** and arrival time distribution **(b)** for the $Aβ_{1-42}$ at a *z/n* ratio of −5/2 (*n* = number of $Aβ_{1-42}$ monomers involved in the formation of the oligomer). The peaks in **(b)** are due to oligomers with even numbers of monomer components, the smallest of which would be the dimer with five negative charges. The arrival time distributions are complex and indicate the presence of $Aβ_{1-42}$ dimers, tetramers, hexamers and dodecamers are present. Adapted by permission from Springer Nature Customer Service Centre GmbH: Springer Nature, Ref. [155], Copyright (2019).

Ion mobility spectrometry (IMS) allows the simultaneous characterization of different conformational states of Aβ oligomers and can lead to an enhanced understanding of the mechanism by which small molecules modulate and/or inhibit amyloid formation. Changes in Aβ conformation with the concomitant appearance or disappearance of different oligomeric states can be monitored over time, with a distinct advantage over complementary biophysical techniques (CD, NMR, and FT-IR) which yield population-average data [156].

A representative application of IM–MS is reported in the work by Lee *et al.* on the development of a novel promising anti-Aβ compound named ML [109]. The capacity of ML to inhibit *in vitro* amyloid aggregation was demonstrated by IM–MS analysis. The ATD of the *z/n* = −5/2 peak of $Aβ_{1-42}$ alone (Figure 12a) exhibited four signals assigned as dimer, tetramer, hexamer and dodecamer; $Aβ_{1-42}$ treated with ML showed a lower signal intensity of the feature due to the hexamer, while the dodecamer was not observed (Figure 12b). These results indicate that the formation of hexamer and dodecamer is inhibited by ML. This has been considered a promising result, since the $Aβ_{1-42}$ dodecamer is considered a key neurotoxic intermediate in the fibril formation. $Aβ_{1-42}$ dodecamer, indeed, was previously observed to seed the formation of extended, linear pre-protofibrillar

β-sheet structures and has been identified as neurotoxic in AD brain and in transgenic mice [157-159]. IM–MS was also used to assess the ability of ML to disaggregate Aβ$_{1-42}$ pre-formed dodecamers (Figure 12c and d).
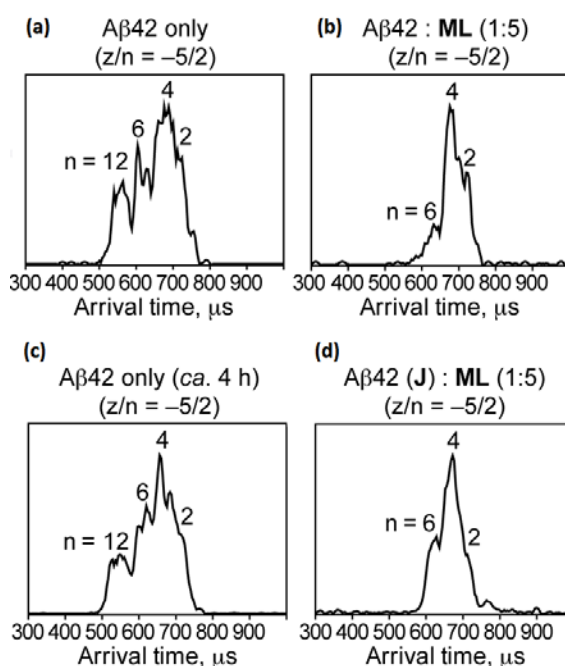

Figure 12. ATD profiles for **(a)** pure Aβ$_{1-42}$ and **(b)** 1:5 mixture of Aβ$_{1-42}$ and ML sample, respectively. **(c)** ATD for the z/n = −5/2 peak of the Aβ$_{1-42}$ sample prepared and placed on ice for ca. 4 h and (d) ATD for the z/n = −5/2 peak of the pre-incubated Aβ$_{1-42}$ sample immediately following the addition of ML (ca. 5 min). Adapted with permission from Ref. [109]. Copyright (2014) American Chemical Society.

A similar approach was fruitfully employed by Zheng *et al.* to investigate the effect of molecular tweezers on Aβ$_{1-42}$ self-assembly [160]. Downey *et al.* employed IM–MS to experimentally assay the efficacy of new molecule computationally designed and incorporating structural characteristics of known Aβ inhibitors [155]. IM–MS analysis was also used to investigate the effects of two modified Aβ$_{39-42}$ derivatives on the early assembly of Aβ$_{1-42}$ [161]. Finally, Kocis exploited IM–MS to evaluate the anti-aggregating activity of tramiprosate [113].

A novel MS-based approach to study Aβ oligomerization was proposed in 2012 by Cernescu *et al.* [162] and recently exploited by Stark *et al.* [141]. It is based on the use of the laser-induced liquid bead ion desorption (LILBID)-MS in which desorption of the analyte from micro-droplets is induced by irradiation with mid-IR laser pulses. Under optimized conditions, this method preserves specific protein−protein interactions and allows monitoring the oligomerization process of Aβ up to 20-mers. As reported by Stark, LILBID-MS could also be

fruitfully employed to assess the inhibition capacity of the newly-synthesized peptidomimetic compound 18 toward Aβ$_{1-42}$ aggregation [141].
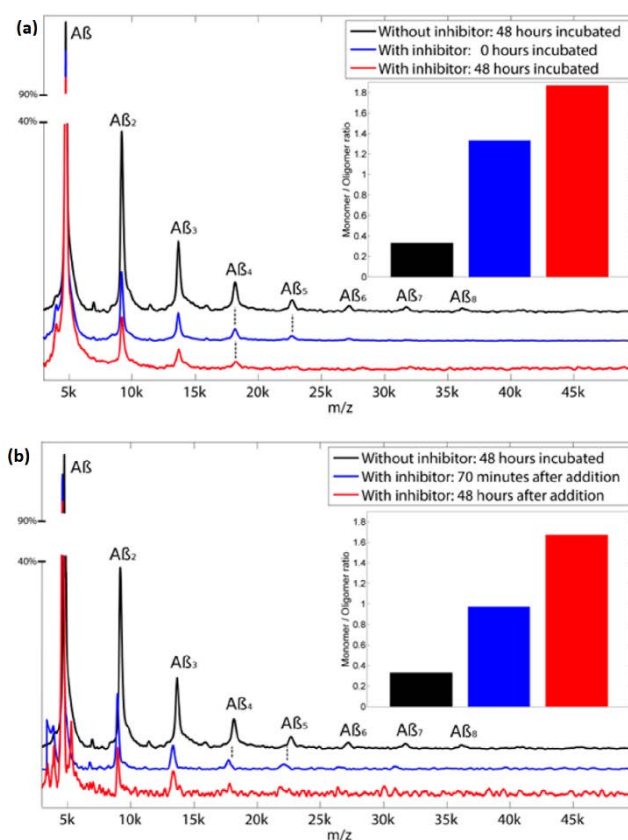
Figure 13. (a) LILBID-MS spectra of Aβ$_{1-42}$ (100 µM) with and without a 4-fold excess of inhibitor (compound 18). The sample was incubated for 48 h at 4 °C. The inlet shows the monomer/oligomer ratios for these spectra. **(b)** LILBID-MS spectra of an Aβ$_{1-42}$ sample (100 µM) incubated for 48 h at 4 °C (black) and treated afterward with 400 µM inhibitor 18 for 70 min (blue) and 48 h (red). The different Aβ$_{1-42}$ oligomers are indicated. The inlet shows the monomer/oligomer ratio for those three spectra. Adapted with permission from Ref. [141]. Copyright (2017) American Chemical Society.

When Aβ$_{1-42}$ aggregation occurs, signals for oligomer species up to 8-mer could be detected; on the other hand, the spectra for the freshly dissolved samples, as well as for Aβ$_{1-42}$ samples incubated with compound 18, showed mainly monomeric Aβ with small amounts of dimers, trimers, tetramers and pentamers (Figure 13a). The LILBID-MS analysis not only confirmed the anti-aggregating activity of compound 18 but also showed its capacity to partially reverse the aggregation process (Figure 13b).

Identifying protein–ligand interactions is a key step during early-stage drug discovery [163]. The assessment of the interaction of anti-Aβ agents with Aβ peptides provides important information on their mechanism of action [152, 164]. Notwithstanding, some Aβ inhibitors are capable to covalently bind Aβ peptides, most of the tested compounds are involved in noncovalent interactions. MS analysis of non-covalent interactions has recently been applied to this field, since recent advances enable the determination of the molecular mass of protein–ligand complexes without the disruption of non-covalent interactions. This approach is called "native MS" or "MS under non-denaturing conditions" [165]. Native MS is considered a powerful diagnostic tool since, along with the detection of non-covalent complexes, it allows the identification of the sites involved in the interaction upon isotope or covalent labeling (see work by Liu *et al.* on the amyloidogenic beta-2 microglobulin [166]) and provides a measure of association ratios and interaction strengths [167]. Native MS has been successfully used to study the interaction between Aβ and transition metal ions (Cu^{2+}, Zn^{2+}, Ir^{3+}) and anti-Aβ active compounds [167-170].

IM–MS analysis allows the preservation of non-covalent protein–ligand complexes, so that the binding interactions of small molecules to target peptides can be observed concomitantly with changes in the relative abundances and distributions of oligomeric species. These changes can be directly correlated to alterations of the fibril formation rate or yield and allow the identification of novel inhibitors. Moreover, IM–MS can be used for HTS binding assays, with a rate of up to 5000 molecules per day [109, 113, 152, 161, 164, 171].

An interesting work exploiting IM–MS to analyze the mode of interaction of a series of small molecules with $Aβ_{1-40}$ was reported by Young *et al.* [152]. The interaction of $Aβ_{1-40}$ with three inhibitors of Aβ aggregation, tramiprosate, hemin and epigallocatechin gallate (EGCG), was investigated [172-174]. IM–MS unveiled the nature of the interaction of the tested compounds with $Aβ_{1-40}$. In particular, the analysis showed that no interaction occurred between $Aβ_{1-40}$ and hemin (Figure 14c), while a non-specific interaction was detected for tramiprosate, which was capable of multiple binding to the triply- and quadruply-charged $Aβ_{1-40}$ monomer (Figure 14b). As a result, neither tramiprosate nor hemin were able to inhibit amyloid fibril formation (Figure 14e–f). Conversely, EGCG specifically bound $Aβ_{1-40}$ (Figure 14d) forming a 1:1 complex which resulted in the formation of amorphous aggregates (Figure 14e–f). These results highlight how a specific binding to $Aβ_{1-40}$ is crucial for the inhibition of amyloid aggregation.
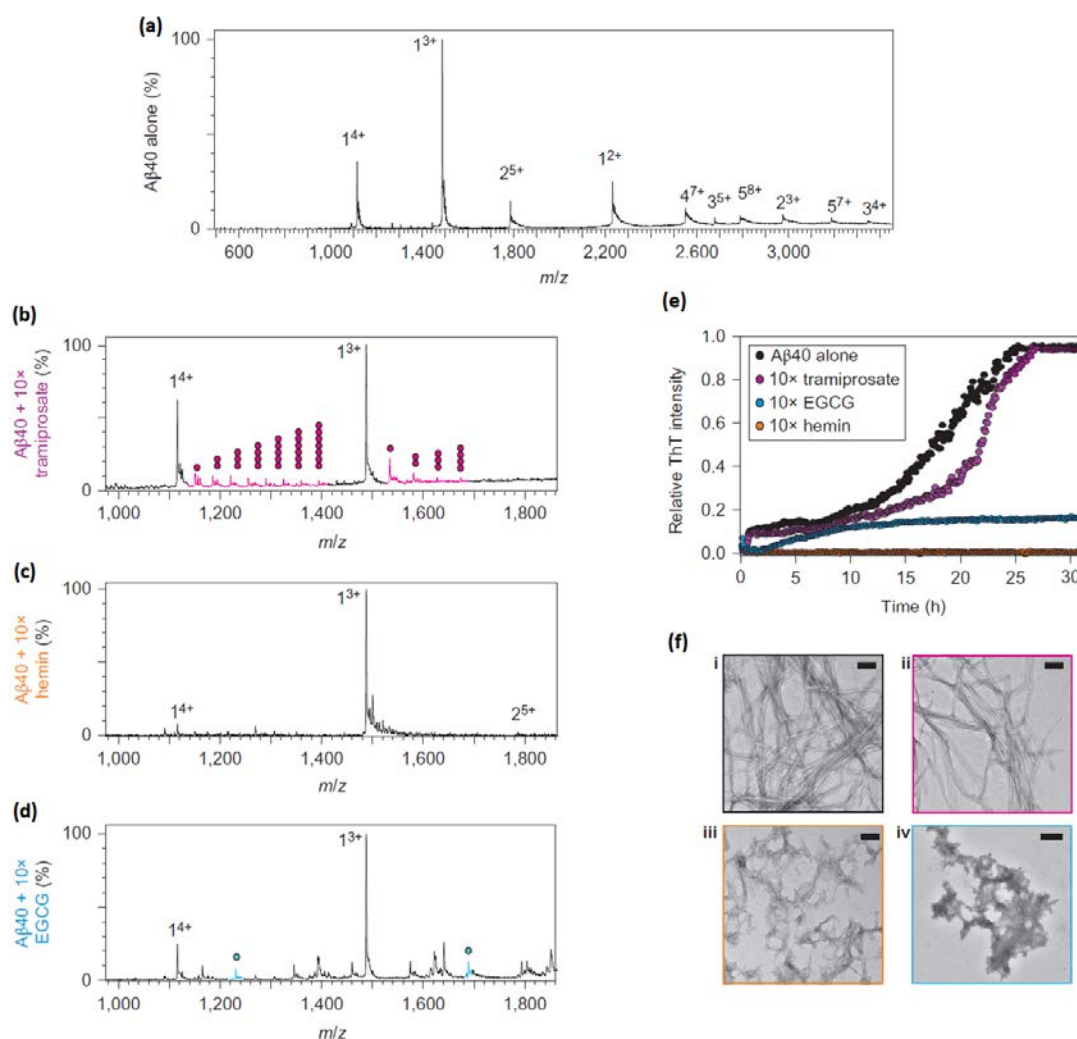
Figure 14. ESI mass spectrum of **(a)** Aβ$_{1-40}$ (numbers adjacent to the peaks denote oligomer order, with the positive charge state of the ions in superscript). Positive-ion ESI mass spectra of Aβ$_{1-40}$ (32 μM) incubated in the presence of **(b)** 320 μM tramiprosate, **(c)** 320 μM hemin or **(d)** 320 μM EGCG. **(e)** ThT fluorescence intensity of Aβ$_{1-40}$ alone (black circles) in the presence of tramiprosate (pink circles), EGCG (blue circles) or hemin (orange circles) at molecule: Aβ$_{1-40}$ molar ratios of 10:1. **(f)** Negative-stain TEM images of Aβ$_{1-40}$ alone **(i)** or incubated with 10:1 molar ratios of tramiprosate **(ii)**, hemin **(iii)** or EGCG **(iv)** (five days, 25 °C, quiescent). Scale bars: 100 nm. Adapted by permission from Springer Nature Customer Service Centre GmbH: Springer Nature, Ref. [152], Copyright (2015).

3.3 Covalent modifications of target proteins

The currently available MS-based methodologies are considered the most suitable for the analysis of protein covalent modifications. MS analysis provides high accuracy, sensitivity and unbiased identification of modified residues, along with quantitative information [175]. The covalent modifications affecting the structure of proteins can be assessed by top-down and bottom-up approaches, which are often used in combination, unveiling complementary information. Generally, the top-down approach is at first employed for the detection

of the global pattern of modifications affecting the target protein [176, 177], while the bottom-up one allows the identification of specific residues involved in the covalent modification [177, 178]. These studies are preferentially performed taking the advantages of the currently available high-resolution mass spectrometry (HR-MS)-based methodologies, which allow unbiased identifications.

A workflow including both the top-down and bottom-up approaches was reported by Taniguchi et al., who proposed a promising therapeutic approach to counteract Aβ aggregation based on the photo-oxygenation of Aβ$_{1-42}$ using riboflavin (vitamin B2) catalysis and visible light irradiation under physiological conditions (pH 7.4, 37°C) [177]. At first, MALDI-time-of-flight (MALDI-TOF) MS was exploited to monitor the yield of Aβ$_{1-42}$ oxygenation at selected times. Afterwards, the use of MS allowed the fine characterization of the structural changes induced by the oxidative reaction; indeed, MALDI-TOF analyses performed on Aβ$_{1-16}$, Aβ$_{17-28}$ and Aβ$_{29-42}$, obtained by digestion with the endoproteinase Arg-C, showed that oxygenation affected mainly Aβ$_{1-16}$. Finally, the combined use of ESI-quadrupole-time-of-flight (ESI-QTOF) LC–ESI-MS/MS analyses allowed the identification of Tyr^{10}, His^{13}, His^{14} and Met^{35} as the sites of the oxidative modifications.

A very recent work has reported on the use of ESI-MS for the assessment of the interaction between Aβ$_{1-42}$ and promising anti-Aβ agents belonging to the class of carbon monoxide-releasing molecules (CORM) [88]. In detail, a top-down approach was exploited for the relative quantification of the adduct between Aβ$_{1-42}$ and compound CORM-3, while a bottom-up strategy was used to identify the Aβ$_{1-42}$ residues involved in this interaction. Finally, ESI-MS flow injection analyses were employed to monitor the Aβ$_{1-42}$ monomer abundance over time which offers an estimation of the rate of formation of insoluble fibrils.

3.4 Ligand fishing

Medicinal plants still represent an important source of novel drug leads. Indeed, several medicinal plants in crude form, or their isolated active compounds, have shown to reduce pathological features associated with AD [179-181]. However, the identification of bioactive constituents is a critical and challenging step due to the chemical complexity of natural extracts. Bioassay-guided fractionation of natural extracts has been the mainstream method to identify bioactive compounds, but this approach shows several drawbacks, such as the long and laborious procedures and the possible loss of scarcely abundant active compounds [182].

In this context, the combined use of affinity-based techniques, such as ligand fishing, and MS has gained increasing interest. Ligand fishing exploits the selective binding of compounds to their targets for their isolation and identification. Different approaches have been used for the ligand fishing experiments including magnetic

beads, equilibrium dialysis and ultrafiltration; the most exploited analytical approach for ligand identification, however, is MS, often coupled to LC separation [183]. Concerning AD drug discovery, in recent years, ligand fishing-based workflows entailing the immobilization of target enzymes (AChE and monoamine oxidases) have been developed for the identification of new bioactive compounds [182, 184, 185]; a noteworthy example is the online approach developed by Wang *et al.* [182]. The online ligand fishing platform based on an immobilized capillary AChE-based reactor is particularly attractive since the incubation, ligand isolation and LC–MS analysis were carried out in an automated fashion, greatly enhancing the screening efficiency.

3.5 Evaluation of target enzyme activity

MS is considered a valid alternative to in-solution assays to monitor the activity of enzymes including those involved in AD progression. MS detection is particularly fruitful when the reference substrate is a peptide and the enzymatic reaction involves either a covalent modification or a cleavage. In comparison with fluorescent or colorimetric assays, MS represents a sensitive, fast, and label-free technique which requires low amount of sample; the latter feature is particularly advantageous when highly expensive recombinant proteins or peptides are used in the assay.

A label-free MS assays recently proposed for the HTS of compounds capable of modulating the activity of sirtuin 1 (SIRT1), a nicotinamide adenine dinucleotide (NAD) deacetylase implicated in age-related diseases [186]. In the optimized experimental conditions, the assay mixture containing the substrate of SIRT1, a 21-residued peptide containing the acetylated Lys^9 of the *N*-terminal portion of histone H3 (H3K9), was directly analyzed by ESI-MS and the enzyme activity was calculated from the H3K9 acetylation degree. In the same year, Peng *et al.* developed a new analytical approach for the evaluation of AChE activity and its inhibition based on the use of acetylcholine-d_4 as a surrogate substrate. The catalysis rate could be determined by monitoring the formation of the reaction product, choline-d_4, by LC–ESI-MS/MS [187].

A MS-based analytical approach for the evaluation of GSK-3β inhibitors was recently presented by De Simone *et al.* [188], who assayed enzyme activity and inhibition by determining the phosphorylation degree of the substrate, the glycogen synthase muscle (GSM) peptide. In 2017, Schejbal *et al.* proposed a novel capillary electrophoresis (CE)-MS method for the screening of BACE1 inhibitors [189]: BACE1 activity was assessed by MS using a substrate peptide which contains the cleavage sequence, and monitoring the formation of a shorter peptide (in the presence of an internal standard) derived from the enzymatic reaction. A fast and label-

free MS approach based on direct analysis by MALDI-TOF-MS of product peptides in the presence of an internal standard was recently proposed by Machálková *et al.* [190] for the HTS of BACE1 inhibitors.

4. Microscopy-based methods

Single-molecule biophysical techniques can help visualizing molecular intermediates, monitoring molecular-scale events in real time and measuring a wide range of intermolecular interactions. Microscopy-based methods, such as transmission electron microscopy (TEM), scanning electron microscopy (SEM), laser scanning microscopy (LSM), confocal laser scanning microscopy (CLSM) and atomic force microscopy (AFM) have been all applied to the field of drug discovery for AD; in this context, the vast majority of the recent applications of microscopy-based methods involve the *in vitro* investigation on tau and amyloid aggregation; based on our search criteria, electron microscopies were employed for the *in vivo* or *ex vivo* investigation of morphological alterations on cells or animal tissues in just 4 publications over the last 5 years (3 for TEM, 1 for SEM). In most drug discovery-driven publications, microscopies have been applied conjointly to other in solution techniques, such as fluorescence-based assays and CD studies. Table 3 summarizes the main characteristics of the microscopy-based techniques used in AD drug discovery.

Table 3. Main characteristics of the microscopy-based techniques used in drug discovery for AD.

Technique	Visualization	Sample	Image	Study	Use for qualitative assessment	Use for quantitative assessment
TEM	Negative staining	Dried	2D	Static	High	Scarce
SEM	Sample coating	Dried	2D	Static	Scarce	None
LSM/CLSM	Fluorescent labeling or intrinsic fluorescence	Dried	3D	Static	Low	Scarce
AFM	No labeling or staining required	Dried (in air) or in solution	3D	Static (in air) or dynamic (in solution, high-speed)	Low	Low/Medium

4.1 Transmission electron microscopy (TEM)

TEM is a static imaging tool that is used either alone or, most often, in combination with other high-throughput, in-solution detection methods to image structures at nanometer resolution. In TEM, an electron beam, emitted by a cathode ray source, is focused on an electron-transparent specimen. The electrons transmitted through the specimen generate an image which gives information about the structure of the specimen. Negative staining of the macromolecular structures by a contrast-enhancing stain reagent is usually applied to visualize the target of interest; studies are carried out on dried samples [191]. As other imaging techniques employed in AD drug discovery, TEM has been used to: (a) retrieve morphological information on a molecular target of interest, in order to understand pathological mechanisms; (b) evaluate the effect of a new active compound on

the specific target, which could be either a single target molecule (generally aggregated proteins), cells or tissues.

Likely due to the simplicity of sample preparation (when *in vitro* studies are carried out on protein aggregates, a small aliquot of the sample is deposited onto a proper grid, dried and stained) and the ease of access to TEM instrumentation in most research centers, the number of publications which include a TEM study is quite high: 176 articles published in the last 5 years were found by searching the words "TEM", "Alzheimer" and "treatment" in the abstract (Scopus).

In AD drug discovery, this technique has been mostly used to visualize Aβ and tau aggregates in the absence and in the presence of a candidate inhibitor. In few cases, TEM has also been used to visualize morphological alterations in cells and tissues upon administration of a potential drug candidate to animal models.

Studies on Aβ represent the most common application, with more than 100 articles involving TEM (Scopus). Indeed, the visualization of the eventual formation of amyloid fibrils allows assessing the anti-aggregating properties of a new inhibitor and excluding false positive results, which may arise from optical interference when a fluorescence dye like ThT is used. Some morphology-related considerations can be also drawn when recent instruments with a sufficiently high resolution are used. Also, some quantitative considerations can be made by evaluating fibril density from the TEM images of individual samples. However, quantitative studies are quite limited and most published works use TEM for the qualitative assessment of the presence or absence of aggregates upon treatment.

TEM has been also used to investigate the disaggregating properties of candidate anti-Aβ agents. In this case, a slightly different experimental set up is used, in which Aβ is aggregated prior to the addition of the tested disaggregating agent. TEM images are acquired before the addition (fibrils are formed at this stage) and after a suitable incubation time. Comparison of images acquired in the absence and in the presence of the compound under evaluation allows confirming or excluding disaggregating properties. In most cases, the ThT fluorescence-based assay and TEM are carried out in parallel for this purpose.

Although the number of publications involving TEM imaging of amyloid aggregation is high (> 100), the scope of TEM application and the employed protocols are very similar among studies, and results are mostly discussed in terms of qualitative evaluation. Hence, a bare list of manuscripts published in the last five years in this field would provide, in our opinion, no additional benefit to the readers, who can refer to the most recent literature (15 manuscripts published in the first 5 months of 2019) [89, 192-205] to get general information on the most frequent approaches and protocols. Indeed, the most critical part is not the preparation of TEM grids

and acquisition of TEM images, but the definition of a reliable protocol for reproducible fibrillization of amyloid peptides.

TEM studies for the identification of anti-aggregating compounds toward tau protein and those on anti-Aβ agents share the same objectives, i.e., providing proof of the anti-aggregating properties of a new anti-aggregating agent [33, 97, 206-211] or highlighting its disaggregating properties on pre-formed fibrils [209, 211]. The use of TEM imaging to investigate tau is the subject of a review article by Huseby and Kuret published in 2016 [212]; for tau aggregates preparation and detection, readers can also refer to a method article by Nanavaty *et al.* published in 2017 [213], in which the authors describe protocols for the *in vitro* tau aggregation as well as analytical methods for aggregate analysis including TEM, among others.

TEM analysis is usually carried out as an end-point analysis upon *in vitro* aggregation. Either the full-length protein, its truncated isoforms or the hexapeptide core fragment [306]VQIVYK[311] (PHF6), located in the third repeat of the microtubule-binding region of the tau protein [214], have been used for such studies. In a limited amount of studies, TEM has been used for imaging the cellular ultrastructural changes characteristic of AD and the attenuation of these alterations upon treatment with synthetic agents or natural extracts [215-217]. In particular, Gao *et al.* stained and imaged ultrathin slices of the hippocampus of an Alzheimer rat model to investigate the attenuation of brain alterations upon treatment with gineposide [218], while Zaky *et al.* used TEM to analyze rat brain cortexes and assess the therapeutic effects of a combination of resveratrol and curcumin toward aluminum-induced neuroinflammation [219].

4.2 Scanning electron microscopy (SEM)

SEM is a type of electron microscopy in which a beam of high-energy electrons is scanned over a specimen. Most commonly, a sample image is generated by collecting the secondary electrons emitted by atoms upon the excitation by the electron beam (primary electrons). Since the intensity of secondary electrons emitted by biological materials is too low to create an image, samples are coated with a very thin layer of metal before the analysis to facilitate emission. Furthermore, the specimen is completely dried since water vaporization interferes with image clarity [220]. The use of SEM to investigate common targets in AD is limited: SEM was used to assess the *in vivo* activity of a naphthoquinone-tryptophan derivative on a transgenic model for tauopathies. Overexpression of human tau in *Drosophila* triggers neurodegeneration which can be monitored in the *Drosophila* eyes ('rough eye' phenotype); SEM examination of eye defects in flies treated or untreated with the tested compound was used by Frenkel-Pinter *et al.* to assess the *in vivo* anti-tau properties [206].

Prior to SEM analysis, flies were fixed in 4% paraformaldehyde, washed, dehydrated with ethanol, critical-point dried and coated with gold.

4.3 Laser scanning microscopy (LSM) and confocal LSM (CLSM)

In LSM, a laser light is focused on small spots (0.5 µm) of the specimen. This enables the detection of low concentrations of a fluorescent substance [221]. LSM provides high-contrast images, even with weakly fluorescent dyes. Confocal LSM allows the visualization of multiple focal layers within the specimen and the reconstruction of a three-dimensional image. Furthermore, phase contrast and fluorescence images taken from the same area can be compared and combined enabling a multi-parameter analysis.

In the field of AD drug discovery, LSM has been recently used by Hossain *et al.* to investigate the anti-aggregating properties of asiaticoside, the major triterpene glycoside in *Centella asiatica* [140]. In particular, the authors used two different approaches to visualize the inhibition of amyloid aggregation. In the first one, the authors imaged amyloid fibrils formed in the absence and in the presence of asiaticoside upon staining with the fluorescent dye ThT; in the second approach, they used a mixture of 5-carboxytetramethylrhodamine (TAMRA)-labeled and unlabeled $A\beta_{1-42}$. The measurement of the area of fluorescent spots allowed an estimation of the inhibitory activity; for quantitative purposes, however, the use of in-solution studies would be more accurate, as they give an overall quantitation of the number of fibrils in the whole sample.

Different studies involving the use of CLSM have been published in the last five years. In the work by Stark *et al.* [141], the authors used a double staining strategy: a mixture of unlabeled and Cy5-labeled amyloid peptide ([$A\beta$]/[Cy5-$A\beta$] ratio = 200:1) was used to generate amyloid aggregates, then ThT was added (emission recorded in the 480–630 nm range, λ_{exc} = 458 nm). Quantitative analyses were carried out upon collapsing the *z*-stack into one picture and analyzing the emission of the two dyes independently. In the work by Shanmuganathan *et al.*, CLSM was used to visually assess the anti-aggregating and disaggregating properties of α-bisabolol toward pre-formed $A\beta_{25-35}$ fibrils stained with ThT [222]. This work is the continuation of a study by the same group on active phytocomponents from the marine seaweed *Padina gymnospora*. Indeed, in 2015, CLSM (in the presence of ThT) and TEM were applied to assess the anti-aggregating properties of the acetone extracts from *P. gymnospora* toward $A\beta_{25-35}$ [136]. The same year, CLSM was used in combination with in-solution fluorescence assay and FT-IR spectroscopy to study the anti-aggregating properties of extracts from the marine red alga *Gelidiella acerosa* toward $A\beta_{25-35}$ [223]. Finally, Ma *et al.* used CLSM to assess the protective effects of the monoterpene glycoside paeoniflorin against okadaic acid-induced

hyperphosphorylation of tau in SH-SY5Y cells; in this work, the microtubule-associated protein 2 (MAP-2) and beta III-tubulin were visualized as markers of neuron microtubule damage [217].

<u>4.4 Atomic force microscopy (AFM)</u>

AFM is a scanning probe microscopy technique, in which a tip attached to a flexible cantilever scans the sample surface. The force between the tip and the sample is measured by monitoring the deflection of the cantilever. The vertical movement of the tip generates the surface contour and a topographic map of the sample is generated [224]. Beside topographical images at sub-nanometer resolution, AFM can also probe interactions at a single-molecule level under physiologically relevant conditions; this feature is obviously of great importance in biomedical studies and in drug discovery, for which conditions close to the physiological or pathological ones are desirable.

Applications of AFM in the biomedical field have been reviewed by Mayer *et al.* in 2016 [225]. In drug discovery for AD, AFM imaging has been frequently useful to understand aggregation phenomena at the nanoscale level, as well as to detect interference by active compounds. In its simplest application, AFM can be performed in air with dry samples to visualize protein assemblies, either amyloid or tau, upon their aggregation *in vitro*, helping scientists to distinguish between aggregates with different morphology and aggregate families, i.e., stable oligomers, protofilaments, and fibrils. As for other imaging techniques, the use of multiple techniques may help elucidating the whole process [149]. Further information on the effect of the inhibitor can be also retrieved by measuring the major and minor axes of fibrils and the number of aggregates (Figure 15). This approach can give further hints on the possible mechanism of action of the tested compound, in combination with other studies.

Either amyloid or tau aggregates have been structurally characterized by AFM operating in air, thus using dehydrated, pre-aggregated samples. Concerning the amyloid peptide, AFM has been applied to the investigation of the anti-aggregating properties of a wide variety of compounds, both synthetic and from natural sources [69, 80, 155, 196, 226-253]. In comparison to TEM, the number of AFM applications is more limited, likely because of the lower availability of AFM instruments, the higher level of expertise required for a proper sample preparation and the longer acquisition times.

AFM has been used to investigate tau aggregation and its inhibition to a smaller extent, likely because the recombinant tau isoforms/fragments required to perform *in vitro* studies have become available only recently. Similarly to what observed for TEM-based studies, AFM has been used to visualize aggregates formed by

different tau forms, including the full-length human recombinant protein 2N4R (Figure 15) [254, 255], the 4R0N isoform [209], the htau(244–372) fragment [241] and the AcPHF6 hexapeptide [98, 256].
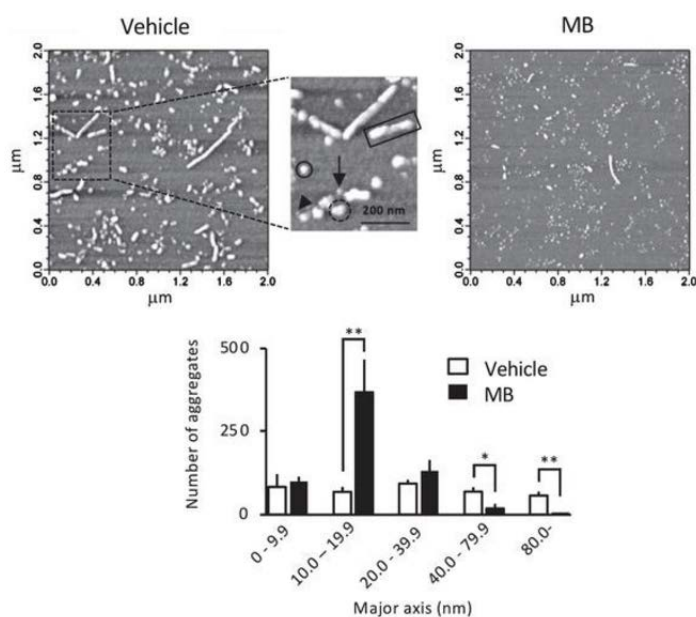
Figure 15. Inhibition of tau fibril formation by methylene blue (MB) as determined by AFM. AFM images were obtained from different areas (2 × 2 μm) of the mica surface and the number and size of tau aggregates was quantitated using a MATLAB-based image analysis program. Reprinted from *Journal of Alzheimer's Disease*, vol. 68, Y. Soeda *et al.* [255]. Copyright (2019), with permission from IOS Press.

As recent examples (2019), in the works by Phan *et al.* [257], Sharma *et al.* [252] and Huang *et al.* [196] AFM was used to retrieve information on fibril morphology and distribution upon treatment with a new inhibitor, in the attempt of better understanding the mechanism of inhibition. Similarly, Downey *et al.* and Siposova *et al.* used AFM to evaluate both the inhibitory and disaggregating properties of the rationally designed compound [AC0107] [155] and the natural polyphenol rottlerin [253], respectively.

The most peculiar applications of AFM are, however, those operating in aqueous solution. This approach allows imaging biological samples and cells in their physiological environment. The more recent advent of high-speed AFM (HS-AFM), which enables probing transient states, has enabled the investigation of dynamic processes such as oligomers formation and their evolution into protofilaments and fibrils. Low-molecular-weight oligomers are thought to be the actual pathological species [258, 259]; the characterization of the formation dynamics of short oligomers is therefore a pivotal step toward the development of diagnostic tools and drug candidates able to prevent or limit these pathologically relevant events. However, the elucidation of

all the amyloid species either targeted or resulting from the inhibitory action of drug candidates is an issue that has been only minimal addressed so far.

The combination of HS-AFM operating in aqueous solution and video-rate data acquisition has allowed visualizing and quantitating this process; the application of this technique in the field of AD drug discovery is still quite limited, although of high interest. In 2016, Watanabe-Nakayama *et al.* used HS-AFM to investigate the dynamics of $A\beta_{1-42}$ assembly and to visualize both initial fibril nucleation and fibril elongation. The authors observed a peculiar bidirectional switching between the spiral and straight growth modes of $A\beta_{1-42}$ [260]. The same approach also allowed monitoring the inhibitory effect of myricetin on the growth of amyloid fibrils over time (Figure 16).
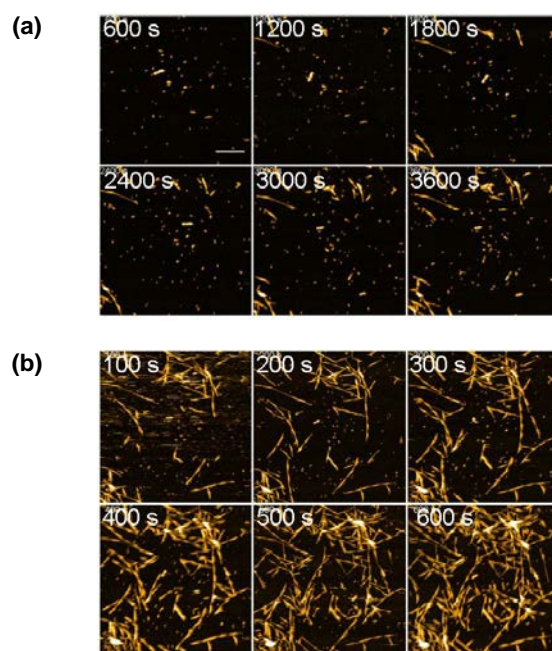
Figure 16. Inhibition of the $A\beta_{1-42}$ fibril growth by myricetin as determined by HS-AFM. **(a)** Serial images of the HS-AFM stage of the reaction mixtures containing $A\beta_{1-42}$ and myricetin. The indicated time corresponds to the elapsed time after the addition of salt for acceleration of fibril growth. **(b)** Serial images of the same surface without of myricetin. The frame rate was 0.2 frames per second and the pixel size was 400 × 400. Scale bar: 300 nm. Adapted from Ref. [260]. Copyright (2016), National Academy of Sciences.

In 2017, Teplow *et al.* published an impressive work in which they used time-lapse HS-AFM to study the dynamics of amyloid oligomers (trimers, pentamers and heptamers, obtained by photochemical cross-linking) in solution [261]. Thanks to the high speed of acquisition, time-lapse HS-AFM enabled the visualization of the structural dynamics of oligomers at nanometer resolution on a millisecond time scale and allowed the authors

to visualize the fluctuation of pentamers and heptamers between single-globular and multi-globular assembly species.

5. Conclusions

The drugs against AD currently available on the market show limited short-term clinical effects for some patients and mild to moderate cholinergic adverse effects in a minority of patients, as well as potentially underappreciated long-term toxicity; This makes the research for new effective drugs an urgent need. In the last few years, new analytical tools have become available to support the discovery of new drugs against AD. Some of these advanced methodologies have the great advantage of exploiting miniaturization facilitating the HTS of compounds for fast hit identification. Other major benefit of such techniques is the ability to allow a reliable and quick identification of positive hits and the rapid definition SARs which is mandatory to tune lead structures to improved activity and bioavailability. Moreover, new approaches focus on a deeper characterization of the mechanisms involved in molecular recognition processes by probing the structure and folding of target proteins and monitoring structural and morphological changes upon binding with ligands.

Significant advances in pre-clinical sciences, with the discovery of new targets and pathogenetic mechanisms, support a certain degree of optimism that effective therapeutic interventions against AD will be found in a not so distant future. In fact, enhanced capabilities in the production of large amounts of high-quality proteins, including membrane proteins, will increase the number of assays in the drug discovery portfolio that can benefit from these methods. The reviewed methodologies provide the necessary analytical tools to ease the discovery of new targets and ligands, showing the fundamental feature of being adaptable to the investigation of diverse target–ligand interactions. We reported the main applications of the discussed techniques in Table 4 in order to make as simple as possible the choice of the appropriate analytical methodology to be adopted to the study of a selected system. We are confident that the application of the new analytical approaches will accelerate the AD discovery process, bringing new active molecules to clinical trials.

Table 4. Summary of the main information to be gained by applying the discussed analytical techniques in AD drug discovery.

Method	Technique	Enzyme inhibition				Protein aggregation				Protein/ligand interaction			
		Qualitative assessment		Quantitative assessment		Qualitative assessment		Quantitative assessment		Qualitative assessment		Quantitative assessment	
		Ligand selection	Mechanism of action	Potency	Affinity	Ligand selection	Mechanism of action	Potency	Affinity	Ligand selection	Mechanism of interaction	Kinetics	Affinity
Spectroscopic	Fluorescence/Luminescence (2.1)	✓	✓	✓	✓	✓		✓		✓	✓		✓
	SPR (2.2)	✓	✓		✓	✓			✓	✓	✓	✓	✓
	CD (2.3)					✓	✓			✓	✓		
	NMR (2.4)	✓	✓	✓		✓	✓			✓	✓		
	FT-IR (2.5)					✓	✓			✓	✓		
	UV-RR (2.6)					✓	✓			✓	✓		
	FCS (2.7)					✓	✓			✓	✓		
MS-based	IM–MS, LILBID-MS (3.1)					✓	✓	✓		✓	✓		
	ESI-MS, MALDI-MS (3.2–3.5)	✓	✓	✓		✓		✓		✓	✓ [a]	✓	
Microscopy-based	TEM (4.1)					✓		✓ [b]					
	LSM/CLSM (4.3)					✓		✓ [b]					
	AFM (4.3)					✓		✓					

(a) Covalent/non-covalent binding. **(b)** These applications are based on the analysis of a suitable number of specimen sections to make the evaluation statistically significant.

References

[1] L.S. Schneider, F. Mangialasche, N. Andreasen, H. Feldman, E. Giacobini, R. Jones, V. Mantua, P. Mecocci, L. Pani, B. Winblad, M. Kivipelto, Clinical trials and late-stage drug development for Alzheimer's disease: An appraisal from 1984 to 2014, J. Intern. Med. 275 (2014) 251–283. https://doi.org/10.1111/joim.12191.

[2] G. Bjørklund, J. Aaseth, M. Dadar, S. Chirumbolo, Molecular targets in Alzheimer's disease, Mol. Neurobiol. 56 (2019) 7032–7044. https://doi.org/10.1007/s12035-019-1563-9.

[3] G.L. Ellman, K.D. Courtney, V. Andres, R.M. Feather-Stone, A new and rapid colorimetric determination of acetylcholinesterase activity, Biochem. Pharmacol. 7 (1961) 88–95. https://doi.org/10.1016/0006-2952(61)90145-9.

[4] H. LeVine, Quantification of beta-sheet amyloid fibril structures with thioflavin T, Methods Enzymol. 309 (1999) 274–284. https://doi.org/10.1016/s0076-6879(99)09020-5.

[5] L. Stryer, R.P. Haugland, Energy transfer: A spectroscopic ruler, Proc Natl Acad Sci U S A 58 (1967) 719–726. https://doi.org/10.1073/pnas.58.2.719.

[6] J.M. Zwier, T. Roux, M. Cottet, T. Durroux, S. Douzon, S. Bdioui, N. Gregor, E. Bourrier, N. Oueslati, L. Nicolas, N. Tinel, C. Boisseau, P. Yverneau, F. Charrier-Savournin, M. Fink, E. Trinquet, A fluorescent ligand-binding alternative using Tag-lite[®] technology, J. Biomol. Screen. 15 (2010) 1248–1259. https://doi.org/10.1177/1087057110384611.

[7] S. Kumar, P. Kellish, W.E. Robinson, D. Wang, D.H. Appella, D.P. Arya, Click dimers to target HIV TAR RNA conformation, Biochemistry (Mosc.) 51 (2012) 2331–2347. https://doi.org/10.1021/bi201657k.

[8] L. Stryer, Exploring light and life, J. Biol. Chem. 287 (2012) 15164–15173. https://doi.org/10.1074/jbc.X112.361436.

[9] C.E. Antal, J.D. Violin, M.T. Kunkel, S. Skovsø, A.C. Newton, Intramolecular conformational changes optimize protein kinase C signaling, Chem. Biol. 21 (2014) 459–469. https://doi.org/10.1016/j.chembiol.2014.02.008.

[10] F. Mancini, A. De Simone, V. Andrisano, Beta-secretase as a target for Alzheimer's disease drug discovery: An overview of *in vitro* methods for characterization of inhibitors, Anal. Bioanal. Chem. 400 (2011) 1979–1996. https://doi.org/10.1007/s00216-011-4963-x.

[11] P. Wu, L. Brand, Resonance energy transfer: Methods and applications, Anal. Biochem. 218 (1994) 1–13. https://doi.org/10.1006/abio.1994.1134.

[12] A. De Simone, C. Seidl, C.A. Santos, V. Andrisano, Liquid chromatographic enzymatic studies with on-line beta-secretase immobilized enzyme reactor and 4-(4-dimethylaminophenylazo) benzoic acid/5-[(2-aminoethyl) amino] naphthalene-1-sulfonic acid peptide as fluorogenic substrate, J. Chromatogr. B Analyt. Technol. Biomed. Life. Sci. 953–954 (2014) 108–114. https://doi.org/10.1016/j.jchromb.2014.01.056.

[13] J. Chlebek, A. De Simone, A. Hošťálková, L. Opletal, C. Pérez, D.I. Pérez, L. Havlíková, L. Cahlíková, V. Andrisano, Application of BACE1 immobilized enzyme reactor for the characterization of multifunctional alkaloids from Corydalis cava (Fumariaceae) as Alzheimer's disease targets, Fitoterapia 109 (2016) 241–247. https://doi.org/10.1016/j.fitote.2016.01.008.

[14]   A. De Simone, M. Naldi, L. Davani, M. Bartolini, V. Andrisano, Immobilized enzyme reactors: An overview of applications in drug discovery from 2008 to 2018, Chromatographia 82 (2019) 425–441. https://doi.org/10.1007/s10337-018-3663-5.

[15]   J. Lee, A.A.S. Samson, J.M. Song, Inkjet printing-based β-secretase fluorescence resonance energy transfer (FRET) assay for screening of potential β-secretase inhibitors of Alzheimer's disease, Anal. Chim. Acta 1022 (2018) 89–95. https://doi.org/10.1016/j.aca.2018.03.033.

[16]   A.C. Newton, Protein kinase C: Poised to signal, Am. J. Physiol. Endocrinol. Metab. 298 (2010) E395–402. https://doi.org/10.1152/ajpendo.00477.2009.

[17]   Y. Baba, Y. Ogoshi, G. Hirai, T. Yanagisawa, K. Nagamatsu, S. Mayumi, Y. Hashimoto, M. Sodeoka, Design, synthesis, and structure-activity relationship of new isobenzofuranone ligands of protein kinase C, Bioorg. Med. Chem. Lett. 14 (2004) 2963–2967. https://doi.org/10.1016/j.bmcl.2004.02.097.

[18]   R.C. Yanagita, Y. Nakagawa, N. Yamanaka, K. Kashiwagi, N. Saito, K. Irie, Synthesis, conformational analysis, and biological evaluation of 1-hexylindolactam-V10 as a selective activator for novel protein kinase C isozymes, J. Med. Chem. 51 (2008) 46–56. https://doi.org/10.1021/jm0706719.

[19]   K. Irie, R.C. Yanagita, Y. Nakagawa, Challenges to the development of bryostatin-type anticancer drugs based on the activation mechanism of protein kinase Cδ, Med. Res. Rev. 32 (2012) 518–535. https://doi.org/10.1002/med.20220.

[20]   N. Ohashi, W. Nomura, N. Minato, H. Tamamura, Screening for protein kinase C ligands using fluorescence resonance energy transfer, Chem. Pharm. Bull. (Tokyo) 62 (2014) 1019–1025. https://doi.org/10.1248/cpb.c14-00419.

[21]   X. Zuo, H. Dai, H. Zhang, J. Liu, S. Ma, X. Chen, A peptide-WS$_2$ nanosheet based biosensing platform for determination of β-secretase and screening of its inhibitors, Analyst 143 (2018) 4585–4591. https://doi.org/10.1039/c8an00132d.

[22]   E. Risse, A.J. Nicoll, W.A. Taylor, D. Wright, M. Badoni, X. Yang, M.A. Farrow, J. Collinge, Identification of a compound that disrupts binding of amyloid-β to the prion protein using a novel fluorescence-based assay, J. Biol. Chem. 290 (2015) 17020–17028. https://doi.org/10.1074/jbc.M115.637124.

[23]   A. Sin-Yee Law, M.C. Yeung, V.W. Yam, A luminescence turn-on assay for acetylcholinesterase activity and inhibitor screening based on supramolecular self-assembly of alkynylplatinum(II) complexes on coordination polymer, ACS Appl. Mater. Interfaces 11 (2019) 4799–4808. https://doi.org/10.1021/acsami.8b18739.

[24]   H.H. Nguyen, S.H. Lee, U.J. Lee, C.D. Fermin, M. Kim, Immobilized enzymes in biosensor applications, Materials 12 (2019) 121. https://doi.org/10.3390/ma12010121.

[25]   C.L. Baird, D.G. Myszka, Current and emerging commercial optical biosensors, J. Mol. Recognit. 14 (2001) 261–268. https://doi.org/10.1002/jmr.544.

[26]   R.A. Copeland, D.L. Pompliano, T.D. Meek, Drug-target residence time and its implications for lead optimization, Nat. Rev. Drug Discov. 5 (2006) 730–739. https://doi.org/10.1038/nrd2082.

[27]   E. Fabini, U.H. Danielson, Monitoring drug–serum protein interactions for early ADME prediction through surface plasmon resonance technology, J. Pharm. Biomed. Anal. 144 (2017) 188–194. https://doi.org/10.1016/j.jpba.2017.03.054.

[28]   C. Bertucci, A. Piccoli, M. Pistolozzi, Optical biosensors as a tool for early determination of absorption and distribution parameters of lead candidates and drugs, Comb. Chem. High Throughput Screen. 10 (2007) 433–440. https://doi.org/10.2174/138620707781996411.

[29]   H.H. Nguyen, J. Park, S. Kang, M. Kim, Surface plasmon resonance: A versatile technique for biosensor applications, Sensors 15 (2015) 10481–10510. https://doi.org/10.3390/s150510481.

[30]   Y.T. Han, K. Kim, G.I. Choi, H. An, D. Son, H. Kim, H.J. Ha, J.H. Son, S.J. Chung, H.J. Park, J. Lee, Y.G. Suh, Pyrazole-5-carboxamides, novel inhibitors of receptor for advanced glycation end products (RAGE), Eur. J. Med. Chem. 79 (2014) 128–142. https://doi.org/10.1016/j.ejmech.2014.03.072.

[31]   J. Li, A.M. Schmidt, Characterization and functional analysis of the promoter of RAGE, the receptor for advanced glycation end products, J. Biol. Chem. 272 (1997) 16498–16506. https://doi.org/10.1074/jbc.272.26.16498.

[32]   A. Bierhaus, S. Schiekofer, M. Schwaninger, M. Andrassy, P.M. Humpert, J. Chen, M. Hong, T. Luther, T. Henle, I. Klöting, M. Morcos, M. Hofmann, H. Tritschler, B. Weigle, M. Kasper, M. Smith, G. Perry, A.M. Schmidt, D.M. Stern, H.U. Häring, E. Schleicher, P.P. Nawroth, Diabetes-associated sustained activation of the transcription factor nuclear factor-κB, Diabetes 50 (2001) 2792–2808. https://doi.org/10.2337/diabetes.50.12.2792.

[33]   P. Lv, C.L. Xia, N. Wang, Z.Q. Liu, Z.S. Huang, S.L. Huang, Synthesis and evaluation of 1,2,3,4-tetrahydro-1-acridone analogues as potential dual inhibitors for amyloid-beta and tau aggregation, Bioorg. Med. Chem. 26 (2018) 4693–4705. https://doi.org/10.1016/j.bmc.2018.08.007.

[34]   Y.T. Han, G.I. Choi, D. Son, N.J. Kim, H. Yun, S. Lee, D.J. Chang, H.S. Hong, H. Kim, H.J. Ha, Y.H. Kim, H.J. Park, J. Lee, Y.G. Suh, Ligand-based design, synthesis, and biological evaluation of 2-aminopyrimidines, a novel series of receptor for advanced glycation end products (RAGE) inhibitors, J. Med. Chem. 55 (2012) 9120–9135. https://doi.org/10.1021/jm300172z.

[35]   G. Yan, L. Hao, Y. Niu, W. Huang, W. Wang, F. Xu, L. Liang, C. Wang, H. Jin, P. Xu, 2-Substituted-thio-*N*-(4-substituted-thiazol/1*H*-imidazol-2-yl)acetamides as BACE1 inhibitors: Synthesis, biological evaluation and docking studies, Eur. J. Med. Chem. 137 (2017) 462–475. https://doi.org/10.1016/j.ejmech.2017.06.020.

[36]   K.R. Valaasani, Q. Sun, G. Hu, J. Li, F. Du, Y. Guo, E.A. Carlson, X. Gan, S.S. Yan, Identification of human ABAD inhibitors for rescuing Aβ-mediated mitochondrial dysfunction, Curr. Alzheimer Res. 2014 (2014) 128–136. https://doi.org/10.2174/1567205011666140130150108.

[37]   Y.H. Wang, K.T. Liou, K.C. Tsai, H.K. Liu, L.M. Yang, C.M. Chern, Y.C. Shen, GSK-3 inhibition through GLP-1R allosteric activation mediates the neurogenesis promoting effect of P7C3 after cerebral ischemic/reperfusional injury in mice, Toxicol. Appl. Pharmacol. 357 (2018) 88–105. https://doi.org/10.1016/j.taap.2018.08.023.

[38]   M. Beeg, M. Stravalaci, M. Romeo, A.D. Carrà, A. Cagnotto, A. Rossi, L. Diomede, M. Salmona, M. Gobbi, Clusterin binds to Aβ$_{1-42}$ oligomers with high affinity and interferes with peptide aggregation by inhibiting primary and secondary nucleation, J. Biol. Chem. 291 (2016) 6958–6966. https://doi.org/10.1074/jbc.M115.689539.

[39] C.J. Dunning, G. McGauran, K. Willén, G.K. Gouras, D.J. O'Connell, S. Linse, Direct high affinity interaction between Aβ42 and GSK3α stimulates hyperphosphorylation of tau. A new molecular link in Alzheimer's disease?, ACS Chem. Neurosci. 7 (2016) 161–170. https://doi.org/10.1021/acschemneuro.5b00262.

[40] I. Park, A.M. Londhe, J.W. Lim, B.G. Park, S.Y. Jung, J.Y. Lee, S.M. Lim, K.T. No, J. Lee, A.N. Pae, Discovery of non-peptidic small molecule inhibitors of cyclophilin D as neuroprotective agents in Aβ-induced mitochondrial dysfunction, J. Comput. Aided Mol. Des. 31 (2017) 929–941. https://doi.org/10.1007/s10822-017-0067-9.

[41] E. Fabini, A. Tramarin, M. Bartolini, Combination of human acetylcholinesterase and serum albumin sensing surfaces as highly informative analytical tool for inhibitor screening, J. Pharm. Biomed. Anal. 155 (2018) 177–184. https://doi.org/10.1016/j.jpba.2018.03.060.

[42] A.R. Wyatt, J.J. Yerbury, R.A. Dabbs, M.R. Wilson, Roles of extracellular chaperones in amyloidosis, J. Mol. Biol. 421 (2012) 499–516. https://doi.org/10.1016/j.jmb.2012.01.004.

[43] A.R. Wyatt, J.J. Yerbury, H. Ecroyd, M.R. Wilson, Extracellular chaperones and proteostasis, Annu. Rev. Biochem. 82 (2013) 295–322. https://doi.org/10.1146/annurev-biochem-072711-163904.

[44] C. Månsson, P. Arosio, R. Hussein, H.H. Kampinga, R.M. Hashem, W.C. Boelens, C.M. Dobson, T.P. Knowles, S. Linse, C. Emanuelsson, Interaction of the molecular chaperone DNAJB6 with growing amyloid-beta 42 (Aβ42) aggregates leads to sub-stoichiometric inhibition of amyloid formation, J. Biol. Chem. 289 (2014) 31066–31076. https://doi.org/10.1074/jbc.M114.595124.

[45] S.I.A. Cohen, P. Arosio, J. Presto, F.R. Kurudenkandy, H. Biverstal, L. Dolfe, C. Dunning, X. Yang, B. Frohm, M. Vendruscolo, J. Johansson, C.M. Dobson, A. Fisahn, T.P.J. Knowles, S. Linse, A molecular chaperone breaks the catalytic cycle that generates toxic Aβ oligomers, Nat. Struct. Mol. Biol. 22 (2015) 207–213. https://doi.org/10.1038/nsmb.2971.

[46] D. Harold, R. Abraham, P. Hollingworth, R. Sims, A. Gerrish, M.L. Hamshere, J.S. Pahwa, V. Moskvina, K. Dowzell, A. Williams, N. Jones, C. Thomas, A. Stretton, A.R. Morgan, S. Lovestone, J. Powell, P. Proitsi, M.K. Lupton, C. Brayne, D.C. Rubinsztein, M. Gill, B. Lawlor, A. Lynch, K. Morgan, K.S. Brown, P.A. Passmore, D. Craig, B. McGuinness, S. Todd, C. Holmes, D. Mann, A.D. Smith, S. Love, P.G. Kehoe, J. Hardy, S. Mead, N. Fox, M. Rossor, J. Collinge, W. Maier, F. Jessen, B. Schürmann, R. Heun, H. van den Bussche, I. Heuser, J. Kornhuber, J. Wiltfang, M. Dichgans, L. Frölich, H. Hampel, M. Hüll, D. Rujescu, A.M. Goate, J.S. Kauwe, C. Cruchaga, P. Nowotny, J.C. Morris, K. Mayo, K. Sleegers, K. Bettens, S. Engelborghs, P.P. De Deyn, C. Van Broeckhoven, G. Livingston, N.J. Bass, H. Gurling, A. McQuillin, R. Gwilliam, P. Deloukas, A. Al-Chalabi, C.E. Shaw, M. Tsolaki, A.B. Singleton, R. Guerreiro, T.W. Mühleisen, M.M. Nöthen, S. Moebus, K.H. Jöckel, N. Klopp, H.E. Wichmann, M.M. Carrasquillo, V.S. Pankratz, S.G. Younkin, P.A. Holmans, M. O'Donovan, M.J. Owen, J. Williams, Genome-wide association study identifies variants at CLU and PICALM associated with Alzheimer's disease, Nat. Genet. 41 (2009) 1088–1093. https://doi.org/10.1038/ng.440.

[47] M. Stravalaci, A. Bastone, M. Beeg, A. Cagnotto, L. Colombo, G. Di Fede, F. Tagliavini, L. Cantù, E. Del Favero, M. Mazzanti, R. Chiesa, M. Salmona, L. Diomede, M. Gobbi, Specific recognition of biologically active amyloid-β oligomers by a new surface plasmon resonance-based immunoassay and an *in vivo* assay in *Caenorhabditis elegans*, J. Biol. Chem. 287 (2012) 27796–27805. https://doi.org/10.1074/jbc.M111.334979.

[48] B. Mannini, R. Cascella, M. Zampagni, M. van Waarde-Verhagen, S. Meehan, C. Roodveldt, S. Campioni, M. Boninsegna, A. Penco, A. Relini, H.H. Kampinga, C.M. Dobson, M.R. Wilson, C. Cecchi, F. Chiti, Molecular

mechanisms used by chaperones to reduce the toxicity of aberrant protein oligomers, Proc Natl Acad Sci U S A 109 (2012) 12479–12484. https://doi.org/10.1073/pnas.1117799109.

[49]   F. Flentge, K. Venema, T. Koch, J. Korf, An enzyme-reactor for electrochemical monitoring of choline and acetylcholine: applications in high-performance liquid chromatography, brain tissue, microdialysis, and cerebrospinal fluid, Anal. Biochem. 204 (1992) 305–310 https://doi.org/10.1016/0003-2697(92)90243-z.

[50]   A. Günther, U. Bilitewski, Characterization of inhibitors of acetylcholinesterase by an automated amperometric flow-injection system, Anal. Chim. Acta 300 (1995) 117–125. https://doi.org/10.1016/0003-2670(94)00352-M.

[51]   A. Roda, P. Rauch, E. Ferri, S. Girotti, S. Ghini, G. Carrea, R. Bovara, Chemiluminescent flow sensor for the determination of Paraoxon and Aldicarb pesticides, Anal. Chim. Acta 294 (1994) 35–42. https://doi.org/10.1016/0003-2670(94)85043-7.

[52]   P. Moris, I. Alexandre, M. Roger, J. Remacle, Chemiluminescence assays of organophosphorus and carbamate pesticides, Anal. Chim. Acta 302 (1995) 53–59. https://doi.org/10.1016/0003-2670(94)00432-L.

[53]   E. Milkani, C.R. Lambert, W.G. McGimpsey, Direct detection of acetylcholinesterase inhibitor binding with an enzyme-based surface plasmon resonance sensor, Anal. Biochem. 408 (2011) 212–219. https://doi.org/10.1016/j.ab.2010.09.009.

[54]   J. Patocka, K. Kuca, D. Jun, Acetylcholinesterase and butyrylcholinesterase–important enzymes of human body, Acta Medica (Hradec Kralove) 47 (2004) 215–228. https://doi.org/10.14712/18059694.2018.95.

[55]   H. Dvir, I. Silman, M. Harel, T.L. Rosenberry, J.L. Sussman, Acetylcholinesterase: From 3D structure to function, Chem. Biol. Interact. 187 (2010) 10–22. https://doi.org/10.1016/j.cbi.2010.01.042.

[56]   C.W. Goh, C.C. Aw, J.H. Lee, C.P. Chen, E.R. Browne, Pharmacokinetic and pharmacodynamic properties of cholinesterase inhibitors donepezil, tacrine, and galantamine in aged and young Lister hooded rats, Drug Metab. Dispos. 39 (2011) 402–411. https://doi.org/10.1124/dmd.110.035964.

[57]   G.D. Fasman, Circular Dichroism and the Conformational Analysis of Biomolecules, Plenum Press, New York, 1996.

[58]   C. Bertucci, M. Pistolozzi, A. De Simone, Circular dichroism in drug discovery and development: An abridged review, Anal. Bioanal. Chem. 398 (2010) 155–166. https://doi.org/10.1007/s00216-010-3959-2.

[59]   G. Pescitelli, L. Di Bari, N. Berova, Application of electronic circular dichroism in the study of supramolecular systems, Chem. Soc. Rev. 43 (2014) 5211–5233. https://doi.org/10.1039/c4cs00104d.

[60]   N.J. Greenfield, Using circular dichroism spectra to estimate protein secondary structure, Nat. Protoc. 1 (2007) 2876–2890. https://doi.org/10.1038/nprot.2006.202.

[61]   R.W. Woody, Theory of Circular Dichroism of Proteins, in: G.D. Fasman (Ed.), Circular Dichroism and the Conformational Analysis of Biomolecules, Plenum Press, New York, 1996, pp. 25–67.

[62]   S.J. Basha, P. Mohan, D.P. Yeggoni, Z.R. Babu, P.B. Kumar, A.D. Rao, R. Subramanyam, A.G. Damu, New flavone-cyanoacetamide hybrids with a combination of cholinergic, antioxidant, modulation of β-amyloid aggregation, and neuroprotection properties as innovative multifunctional therapeutic candidates for Alzheimer's

disease and unraveling their mechanism of action with acetylcholinesterase, Mol. Pharm. 15 (2018) 2206–2223. https://doi.org/10.1021/acs.molpharmaceut.8b00041.

[63]   M. Sun, M. Su, H. Sun, Spectroscopic investigation on the interaction characteristics and inhibitory activities between baicalin and acetylcholinesterase, Med. Chem. Res. 27 (2018) 1589–1598. https://doi.org/10.1007/s00044-018-2174-0.

[64]   F. Kamp, H.A. Scheidt, E. Winkler, G. Basset, H. Heinel, J.M. Hutchison, L.M. Lapointe, C.R. Sanders, H. Steiner, D. Huster, Bexarotene binds to the amyloid precursor protein transmembrane domain, alters its α-helical conformation, and inhibits γ-secretase nonselectively in liposomes, ACS Chem. Neurosci. 9 (2018) 1702–1713. https://doi.org/10.1021/acschemneuro.8b00068.

[65]   Q. Sun, J. Zhao, Y. Zhang, H. Yang, P. Zhou, A natural hyperbranched proteoglycan inhibits IAPP amyloid fibrillation and attenuates β-cell apoptosis, RSC Adv. 6 (2016) 105690–105698. https://doi.org/10.1039/c6ra23429a.

[66]   M. Bartolini, C. Bertucci, M.L. Bolognesi, A. Cavalli, C. Melchiorre, V. Andrisano, Insight into the kinetic of amyloid β (1-42) peptide self-aggregation: Elucidation of inhibitors' mechanism of action, ChemBioChem 8 (2007) 2152–2161. https://doi.org/10.1002/cbic.200700427.

[67]   P. Chang, R.S. Talekar, F. Kung, T. Chern, C. Huang, Q. Ye, M. Yang, C. Yu, S. Lai, R.R. Deore, J. Lin, C. Chen, G.S. Chen, J. Chern, A newly designed molecule J2326 for Alzheimer's disease disaggregates amyloid fibrils and induces neurite outgrowth, Neuropharmacology 92 (2015) 146–157. https://doi.org/10.1016/j.neuropharm.2015.01.004.

[68]   X. Dai, W. Hou, Y. Sun, Z. Gao, S. Zhu, Z. Jiang, Chitosan oligosaccharides inhibit/disaggregate fibrils and attenuate amyloid β-mediated neurotoxicity, Int. J. Mol. Sci. 16 (2015) 10526–10536. https://doi.org/10.3390/ijms160510526.

[69]   H. Xie, Z. Qiao, H. Wang, H. Duan, Y. Yang, C. Wang, Inhibition of β-amyloid peptide self-assembly and cytotoxicity by poly(LVFF-co-β-amino ester), J. Pept. Sci. 21 (2015) 608–614. https://doi.org/10.1002/psc.2784.

[70]   B.I. Lee, S. Lee, Y.S. Suh, J.S. Lee, A. Kim, O. Kwon, K. Yu, C.B. Park, Photoexcited porphyrins as a strong suppressor of β-amyloid aggregation and synaptic toxicity, Angew. Chem. Int. Ed. Engl. 54 (2015) 11472–11476. https://doi.org/10.1002/ange.201504310.

[71]   L. Chang, W. Cui, Y. Yang, S. Xu, W. Zhou, H. Fu, S. Hu, S. Mak, J. Hu, Q. Wang, V. Pui-Yan Ma, T. Chung-Lit Choi, E. Dik-Lung Ma, L. Tao, Y. Pang, M.J. Rowan, R. Anwyl, Y. Han, Q. Wang, Protection against β-amyloid-induced synaptic and memory impairments via altering β-amyloid assembly by bis(heptyl)-cognitin, Sci. Rep. 5 (2015) 10256. https://doi.org/10.1038/srep10256.

[72]   R. Malishev, S. Nandi, S. Kolusheva, Y. Levi-Kalisman, F. Klärner, T. Schrader, G. Bitan, R. Jelinek, Toxicity inhibitors protect lipid membranes from disruption by Aβ42, ACS Chem. Neurosci. 6 (2015) 1860–1869. https://doi.org/10.1021/acschemneuro.5b00200.

[73]   A. Botz, V. Gasparik, E. Devillers, A.R. Hoffmann, L. Caillon, E. Chelain, O. Lequin, T. Brigaud, L. Khemtemourian, (*R*)-α-trifluoromethylalanine containing short peptide in the inhibition of amyloid peptide fibrillation, Biopolymers 104 (2015) 601–610. https://doi.org/10.1002/bip.22670.

[74]   K.B. Batkulwar, A.K. Jana, R.K. Godbole, P. Khandelwal, N. Sengupta, M.J. Kulkarni, Hydralazine inhibits amyloid beta (Aβ) aggregation and glycation and ameliorates Aβ$_{1-42}$ induced neurotoxicity, RSC Adv. 6 (2016) 108768–108776. https://doi.org/10.1039/c6ra20225j.

[75]   A.L. Gillman, J. Lee, S. Ramachandran, R. Capone, T. Gonzalez, W. Wrasidlo, E. Masliah, R. Lal, Small molecule NPT-440-1 inhibits ionic flux through Aβ$_{1-42}$ pores: Implications for Alzheimer's disease therapeutics, Nanomedicine: Nanotechnology, Biology and Medicine 12 (2016) 2331–2340. https://doi.org/10.1016/j.nano.2016.06.001.

[76]   Y. Tu, S. Ma, F. Liu, Y. Sun, X. Dong, Hematoxylin inhibits amyloid β-protein fibrillation and alleviates amyloid-induced cytotoxicity, J. Phys. Chem. B 120 (2016) 11360–11368. https://doi.org/10.1021/acs.jpcb.6b06878.

[77]   Y. Fan, D. Wu, X. Yi, H. Tang, L. Wu, Y. Xia, Z. Wang, Q. Liu, Z. Zhou, J. Wang, TMPyP inhibits amyloid-β aggregation and alleviates amyloid-induced cytotoxicity, ACS Omega 2 (2017) 4188–4195. https://doi.org/10.1021/acsomega.7b00877.

[78]   E. Jameel, P. Meena, M. Maqbool, J. Kumar, W. Ahmed, S. Mumtazuddin, M. Tiwari, N. Hoda, B. Jayaram, Rational design, synthesis and biological screening of triazine-triazolopyrimidine hybrids as multitarget anti-Alzheimer agents, Eur. J. Med. Chem. 136 (2017) 36–51. https://doi.org/10.1016/j.ejmech.2017.04.064.

[79]   Z. Zhao, L. Zhu, H. Li, P. Cheng, J. Peng, Y. Yin, Y. Yang, C. Wang, Z. Hu, Y. Yang, Antiamyloidogenic activity of Aβ42-binding peptoid in modulating amyloid oligomerization, Small 13 (2017) 1602857. https://doi.org/10.1002/smll.201602857.

[80]   B. Ren, M. Zhang, R. Hu, H. Chen, M. Wang, Y. Lin, Y. Sun, L. Jia, G. Liang, J. Zheng, Identification of a new function of cardiovascular disease drug 3-morpholinosydnonimine hydrochloride as an amyloid-β aggregation inhibitor, ACS Omega 2 (2017) 243–250. https://doi.org/10.1021/acsomega.6b00397.

[81]   S. Kumar, A.D. Hamilton, α-Helix mimetics as modulators of Aβ self-assembly, J. Am. Chem. Soc. 139 (2017) 5744–5755. https://doi.org/10.1021/jacs.6b09734.

[82]   S. Kumar, A. Henning-Knechtel, M. Magzoub, A.D. Hamilton, Peptidomimetic-based multidomain targeting offers critical evaluation of Aβ structure and toxic function, J. Am. Chem. Soc. 140 (2018) 6562–6574. https://doi.org/10.1021/jacs.7b13401.

[83]   H. Xie, J. Peng, C. Liu, X. Fang, H. Duan, Y. Zou, Y. Yang, C. Wang, Aromatic-interaction-mediated inhibition of β-amyloid assembly structures and cytotoxicity, J. Pept. Sci. 23 (2017) 679–684. https://doi.org/10.1002/psc.3011.

[84]   S. Kumar, A. Henning-Knechtel, I. Chehade, M. Magzoub, A.D. Hamilton, Foldamer-mediated structural rearrangement attenuates Aβ oligomerization and cytotoxicity, J. Am. Chem. Soc. 139 (2017) 17098–17108. https://doi.org/10.1021/jacs.7b08259.

[85]   K. Murakami, T. Yoshioka, S. Horii, M. Hanaki, S. Midorikawa, S. Taniwaki, H. Gunji, K. Akagi, T. Kawase, K. Hirose, K. Irie, Role of the carboxy groups of triterpenoids in their inhibition of the nucleation of amyloid β42 required for forming toxic oligomers, Chem. Commun. (Camb.) 54 (2018) 6272–6275. https://doi.org/10.1039/c8cc03230k.

[86]   T. Liargkova, N. Eleftheriadis, F. Dekker, E. Voulgari, C. Avgoustakis, M. Sagnou, B. Mavroidi, M. Pelecanou, D. Hadjipavlou-Litina, Small multitarget molecules incorporating the enone moiety, Molecules 24 (2019) 199. https://doi.org/10.3390/molecules24010199.

[87]   J. Xu, Y. Yuan, R. Zhang, Y. Song, T. Sui, J. Wang, C. Wang, Y. Chen, S. Guan, L. Wang, A deuterohemin peptide protects a transgenic caenorhabditis elegans model of Alzheimer's disease by inhibiting $A\beta_{1-42}$ aggregation, Bioorg. Chem. 82 (2019) 332–339. https://doi.org/10.1016/j.bioorg.2018.10.072.

[88]   A. De Simone, M. Naldi, D. Tedesco, A. Milelli, M. Bartolini, L. Davani, D. Widera, M.L. Dallas, V. Andrisano, Investigating *in vitro a*myloid peptide 1-42 aggregation: Impact of higher molecular weight stable adducts, ACS Omega 4 (2019) 12308–12318. https://doi.org/10.1021/acsomega.9b01531.

[89]   Z. Zhu, T. Yang, L. Zhang, L. Liu, E. Yin, C. Zhang, Z. Guo, C. Xu, X. Wang, Inhibiting Aβ toxicity in Alzheimer's disease by a pyridine amine derivative, Eur. J. Med. Chem. 168 (2019) 330–339. https://doi.org/10.1016/j.ejmech.2019.02.052.

[90]   T. Chen, S. Zhu, S. Liu, Y. Lu, L. Zhu, Two nitrogen-containing ligands as inhibitors of metal-induced amyloid β-peptide aggregation, CNS Neurol. Disord. Drug Targets 13 (2014) 166–172. https://doi.org/10.2174/18715273113129990076.

[91]   H. Rajaram, M.K. Palanivelu, T.V. Arumugam, V.M. Rao, P.N. Shaw, R.P. McGeary, B.P. Ross, 'Click' assembly of glycoclusters and discovery of a trehalose analogue that retards Aβ40 aggregation and inhibits Aβ40-induced neurotoxicity, Bioorg. Med. Chem. Lett. 24 (2014) 4523–4528. https://doi.org/10.1016/j.bmcl.2014.07.077.

[92]   S. Tabassum, A.M. Sheikh, S. Yano, T. Ikeue, M. Handa, A. Nagai, A carboxylated Zn-phthalocyanine inhibits fibril formation of Alzheimer's amyloid β peptide, FEBS J. 282 (2015) 463–476. https://doi.org/10.1111/febs.13151.

[93]   M. Tonelli, M. Catto, B. Tasso, F. Novelli, C. Canu, G. Iusco, L. Pisani, A. De Stradis, N. Denora, A. Sparatore, V. Boido, A. Carotti, F. Sparatore, Multitarget therapeutic leads for Alzheimer's disease: Quinolizidinyl derivatives of bi- and tricyclic systems as dual inhibitors of cholinesterases and β-amyloid (Aβ) aggregation, ChemMedChem 10 (2015) 1040–1053. https://doi.org/10.1002/cmdc.201500104.

[94]   L. Zhu, Y. Song, P. Cheng, J.S. Moore, Molecular design for dual modulation effect of amyloid protein aggregation, J. Am. Chem. Soc. 137 (2015) 8062–8068. https://doi.org/10.1021/jacs.5b01651.

[95]   T. Chen, Y. Zhang, Y. Shang, X. Gu, Y. Zhu, L. Zhu, NBD-BPEA regulates Zn^{2+}- or Cu^{2+}-induced Aβ40 aggregation and cytotoxicity, Food Chem. Toxicol. 119 (2018) 260–267. https://doi.org/10.1016/j.fct.2018.03.035.

[96]   A. Mohammadi Karakani, G. Riazi, S.M. Ghaffari, S. Ahmadian, F. Mokhtari, M. Jalili Firuzi, S.Z. Bathaie, Inhibitory effect of corcin on aggregation of 1N/4R human tau protein *in vitro*, Iran. J. Basic Med. Sci. 18 (2015) 485–492. https://doi.org/10.22038/IJBMS.2015.4412.

[97]   A. Belostozky, M. Richman, E. Lisniansky, A. Tovchygrechko, J.H. Chill, S. Rahimipour, Inhibition of tau-derived hexapeptide aggregation and toxicity by a self-assembled cyclic D,L-α-peptide conformational inhibitor, Chem. Commun. (Camb.) 54 (2018) 5980–5983. https://doi.org/10.1039/c8cc01233d.

[98]   A. Gandini, M. Bartolini, D. Tedesco, L. Martinez-Gonzalez, C. Roca, N.E. Campillo, J. Zaldivar-Diez, C. Perez, G. Zuccheri, A. Miti, A. Feoli, S. Castellano, S. Petralla, B. Monti, M. Rossi, F. Moda, G. Legname, A. Martinez, M.L. Bolognesi, Tau-centric multitarget approach for Alzheimer's disease: Development of first-in-class dual glycogen synthase kinase 3β and tau-aggregation inhibitors, J. Med. Chem. 61 (2018) 7640–7656. https://doi.org/10.1021/acs.jmedchem.8b00610.

[99]   D. Marion, An introduction to biological NMR spectroscopy, Mol. Cell. Proteomics 12 (2013) 3006–3025. https://doi.org/10.1074/mcp.O113.030239.

[100]   A.H. Kwan, M. Mobli, P.R. Gooley, G.F. King, J.P. Mackay, Macromolecular NMR spectroscopy for the non-spectroscopist, FEBS J. 278 (2011) 687–703. https://doi.org/10.1111/j.1742-4658.2011.08004.x.

[101]   E. Barile, M. Pellecchia, NMR-based approaches for the identification and optimization of inhibitors of protein–protein interactions, Chem. Rev. 114 (2014) 4749–4763. https://doi.org/10.1021/cr500043b.

[102]   W. Becker, K.C. Bhattiprolu, N. Gubensäk, K. Zangger, Investigating protein–ligand interactions by solution nuclear magnetic resonance spectroscopy, ChemPhysChem 19 (2018) 895–906. https://doi.org/10.1002/cphc.201701253.

[103]   G. Bodenhausen, D.J. Ruben, Natural abundance nitrogen-15 NMR by enhanced heteronuclear spectroscopy, Chem. Phys. Lett. 69 (1980) 185–189. https://doi.org/10.1016/0009-2614(80)80041-8.

[104]   G. Leshem, M. Richman, E. Lisniansky, M. Antman-Passig, M. Habashi, A. Gräslund, S.K.T.S. Wärmländer, S. Rahimipour, Photoactive chlorin e6 is a multifunctional modulator of amyloid-β aggregation and toxicity via specific interactions with its histidine residues, Chem. Sci. 10 (2019) 208–217. https://doi.org/10.1039/c8sc01992d.

[105]   P. Schanda, B. Brutscher, Very fast two-dimensional NMR spectroscopy for real-time investigation of dynamic events in proteins on the time scale of seconds, J. Am. Chem. Soc. 127 (2005) 8014–8015. https://doi.org/10.1021/ja051306e.

[106]   K.J. Korshavn, M. Jang, Y.J. Kwak, A. Kochi, S. Vertuani, A. Bhunia, S. Manfredini, A. Ramamoorthy, M.H. Lim, Reactivity of metal-free and metal-associated amyloid-β with glycosylated polyphenols and their esterified derivatives, Sci. Rep. 5 (2015) 17842. https://doi.org/10.1038/srep17842.

[107]   M. Hanaki, K. Murakami, K. Akagi, K. Irie, Structural insights into mechanisms for inhibiting amyloid β42 aggregation by non-catechol-type flavonoids, Bioorg. Med. Chem. 24 (2016) 304–313. https://doi.org/10.1016/j.bmc.2015.12.021.

[108]   H.J. Lee, R.A. Kerr, K.J. Korshavn, J. Lee, J. Kang, A. Ramamoorthy, B.T. Ruotolo, M.H. Lim, Effects of hydroxyl group variations on a flavonoid backbone toward modulation of metal-free and metal-induced amyloid-β aggregation, Inorg. Chem. Front. 3 (2016) 381–392. https://doi.org/10.1039/c5qi00219b.

[109]   S. Lee, X. Zheng, J. Krishnamoorthy, M.G. Savelieff, H.M. Park, J.R. Brender, J.H. Kim, J.S. Derrick, A. Kochi, H.J. Lee, C. Kim, A. Ramamoorthy, M.T. Bowers, M.H. Lim, Rational design of a structural framework with potential use to develop chemical reagents that target and modulate multiple facets of Alzheimer's disease, J. Am. Chem. Soc. 136 (2014) 299–310. https://doi.org/10.1021/ja409801p.

[110]   J.S. Derrick, R.A. Kerr, K.J. Korshavn, M.J. McLane, J. Kang, E. Nam, A. Ramamoorthy, B.T. Ruotolo, M.H. Lim, Importance of the dimethylamino functionality on a multifunctional framework for regulating metals, amyloid-β, and oxidative stress in Alzheimers disease, Inorg. Chem. 55 (2016) 5000–5013. https://doi.org/10.1021/acs.inorgchem.6b00525.

[111]   M.R. Jones, C. Dyrager, M. Hoarau, K.J. Korshavn, M.H. Lim, A. Ramamoorthy, T. Storr, Multifunctional quinoline-triazole derivatives as potential modulators of amyloid-β peptide aggregation, J. Inorg. Biochem. 158 (2016) 131–138. https://doi.org/10.1016/j.jinorgbio.2016.04.022.

[112] A. Ghosh, N. Pradhan, S. Bera, A. Datta, J. Krishnamoorthy, N.R. Jana, A. Bhunia, Inhibition and degradation of amyloid beta (Aβ40) fibrillation by designed small peptide: A combined spectroscopy, microscopy, and cell toxicity study, ACS Chem. Neurosci. 8 (2017) 718–722. https://doi.org/10.1021/acschemneuro.6b00349.

[113] P. Kocis, M. Tolar, J. Yu, W. Sinko, S. Ray, K. Blennow, H. Fillit, J.A. Hey, Elucidating the Aβ42 anti-aggregation mechanism of action of tramiprosate in Alzheimer's disease: Integrating molecular analytical methods, pharmacokinetic and clinical data, CNS Drugs 31 (2017) 495–509. https://doi.org/10.1007/s40263-017-0434-z.

[114] M. Hanaki, K. Murakami, S. Katayama, K. Akagi, K. Irie, Mechanistic analyses of the suppression of amyloid β42 aggregation by apomorphine, Bioorg. Med. Chem. 26 (2018) 1538–1546. https://doi.org/10.1016/j.bmc.2018.01.028.

[115] K. Pervushin, R. Riek, G. Wider, K. Wüthrich, Attenuated T2 relaxation by mutual cancellation of dipole-dipole coupling and chemical shift anisotropy indicates an avenue to NMR structures of very large biological macromolecules in solution, Proc. Natl. Acad. Sci. U.S.A. 94 (1997) 12366–12371. https://doi.org/10.1073/pnas.94.23.12366.

[116] Z. Wang, Y. Wang, B. Wang, W. Li, L. Huang, X. Li, Design, synthesis, and evaluation of orally available clioquinol-moracin M hybrids as multitarget-directed ligands for cognitive improvement in a rat model of neurodegeneration in Alzheimer's disease, J. Med. Chem. 58 (2015) 8616–8637. https://doi.org/10.1021/acs.jmedchem.5b01222.

[117] M. Mayer, B. Meyer, Characterization of ligand binding by saturation transfer difference NMR spectroscopy, Angew. Chem. Int. Ed. Engl. 38 (1999) 1784–1788. https://doi.org/10.1002/(SICI)1521-3773(19990614)38:12<1784::AID-ANIE1784>3.0.CO;2-Q.

[118] P. Bacalhau, A.A. San Juan, C.S. Marques, D. Peixoto, A. Goth, C. Guarda, M. Silva, S. Arantes, A.T. Caldeira, R. Martins, A.J. Burke, New cholinesterase inhibitors for Alzheimer's disease: Structure activity studies (SARS) and molecular docking of isoquinolone and azepanone derivatives, Bioorg. Chem. 67 (2016) 1–8. https://doi.org/10.1016/j.bioorg.2016.05.004.

[119] T.P.C. Chierrito, S.P. Mantoani, C. Roca, C. Requena, V. Sebastian-Perez, W.O. Castillo, N.C.S. Moreira, C. Pérez, E.T. Sakamoto-Hojo, C.S. Takahashi, J. Jiménez-Barbero, F.J. Cañada, N.E. Campillo, A. Martinez, I. Carvalho, From dual binding site acetylcholinesterase inhibitors to allosteric modulators: A new avenue for disease-modifying drugs in Alzheimer's disease, Eur. J. Med. Chem. 139 (2017) 773–791. https://doi.org/10.1016/j.ejmech.2017.08.051.

[120] T.P.C. Chierrito, S. Pedersoli-Mantoani, C. Roca, V. Sebastian-Pérez, L. Martínez-Gonzalez, D.I. Pérez, C. Perez, A. Canales, F.J. Cañada, N.E. Campillo, I. Carvalho, A. Martinez, Chameleon-like behavior of indolylpiperidines in complex with cholinesterases targets: Potent butyrylcholinesterase inhibitors, Eur. J. Med. Chem. 145 (2018) 431–444. https://doi.org/10.1016/j.ejmech.2018.01.007.

[121] P. Bacalhau, A.A. San Juan, A. Goth, A.T. Caldeira, R. Martins, A.J. Burke, Insights into (*S*)-rivastigmine inhibition of butyrylcholinesterase (BuChE): Molecular docking and saturation transfer difference NMR (STD-NMR), Bioorg. Chem. 67 (2016) 105–109. https://doi.org/10.1016/j.bioorg.2016.06.002.

[122] N.U. Tanoli, S.A.K. Tanoli, A.G. Ferreira, S. Gul, Z. Ul-Haq, Evaluation of binding competition and group epitopes of acetylcholinesterase inhibitors by STD NMR, Tr-NOESY, DOSY and molecular docking: An old approach but new findings, MedChemComm 6 (2015) 1882–1890. https://doi.org/10.1039/c5md00231a.

[123]   P. Bacalhau, L. Fernandes, M. Rosário Martins, F. Candeias, E.P. Carreiro, Ó. López, A. Teresa Caldeira, J. Totobenazara, R.C. Guedes, A.J. Burke, In silico, NMR and pharmacological evaluation of an hydroxyoxindole cholinesterase inhibitor, Bioorg. Med. Chem. 27 (2019) 354–363. https://doi.org/10.1016/j.bmc.2018.12.007.

[124]   N.U. Tanoli, S.A.K. Tanoli, A.G. Ferreira, M. Mehmood, S. Gul, J.L. Monteiro, L.C.C. Vieira, T. Venâncio, A.G. Correa, Z. Ul-Haq, Characterization of the interactions between coumarin-derivatives and acetylcholinesterase: Examination by NMR and docking simulations, Journal of Molecular Modeling 24 (2018) 207. https://doi.org/10.1007/s00894-018-3751-3.

[125]   G.M. Clore, A.M. Gronenborn, Theory and applications of the transferred nuclear Overhauser effect to the study of the conformations of small ligands bound to proteins, J. Magn. Reson. 48 (1982) 402–417. https://doi.org/10.1016/0022-2364(82)90073-7.

[126]   C. Guzzi, L. Colombo, A.D. Luigi, M. Salmona, F. Nicotra, C. Airoldi, Flavonoids and their glycosides as anti-amyloidogenic compounds: Aβ1–42 interaction studies to gain new insights into their potential for Alzheimer's disease prevention and therapy, Chem. Asian J. 12 (2017) 67–75. https://doi.org/10.1002/asia.201601291.

[127]   A.M. Matos, T. Man, I. Idrissi, C.C. Souza, E. Mead, C. Dunbar, J. Wolak, M.C. Oliveira, D. Evans, J. Grayson, B. Partridge, C. Garwood, K. Ning, G. Sharman, B. Chen, A.P. Rauter, Discovery of *N*-methylpiperazinyl flavones as a novel class of compounds with therapeutic potential against Alzheimer's disease: Synthesis, binding affinity towards amyloid β oligomers (Aβo) and ability to disrupt Aβo-PrP C interactions, Pure Appl. Chem. 91 (2019) 1107–1136. https://doi.org/10.1515/pac-2019-0114.

[128]   A. Palmioli, S. Bertuzzi, A. De Luigi, L. Colombo, B. La Ferla, M. Salmona, I. De Noni, C. Airoldi, bioNMR-based identification of natural anti-Aβ compounds in Peucedanum ostruthium, Bioorg. Chem. 83 (2019) 76–86. https://doi.org/10.1016/j.bioorg.2018.10.016.

[129]   A. Gimeno, L.M. Santos, M. Alemi, J. Rivas, D. Blasi, E.Y. Cotrina, J. Llop, G. Valencia, I. Cardoso, J. Quintana, G. Arsequell, J. Jiménez-Barbero, Insights on the interaction between transthyretin and Aβ in solution. A saturation transfer difference (STD) NMR analysis of the role of iododiflunisal, J. Med. Chem. 60 (2017) 5749–5758. https://doi.org/10.1021/acs.jmedchem.7b00428.

[130]   S.F. Da Cunha Xavier Soares, A.A. Vieira, R.T. Delfino, J.D. Figueroa-Villar, NMR determination of *Electrophorus electricus* acetylcholinesterase inhibition and reactivation by neutral oximes, Bioorg. Med. Chem. 21 (2013) 5923–5930. https://doi.org/10.1016/j.bmc.2013.05.063.

[131]   E.D.C. Petronilho, M.D.N. Rennó, N.G. Castro, F.M.R. da Silva, A.D.C. Pinto, J.D. Figueroa-Villar, Design, synthesis, and evaluation of guanylhydrazones as potential inhibitors or reactivators of acetylcholinesterase, J. Enzyme Inhib. Med. Chem. 31 (2016) 1069–1078. https://doi.org/10.3109/14756366.2015.1094468.

[132]   D.C. Ferreira Neto, M. De Souza Ferreira, E. Da Conceição Petronilho, J. Alencar Lima, S. Oliveira Francisco De Azeredo, J. De Oliveira Carneiro Brum, C. Jorge Do Nascimento, J.D. Figueroa Villar, A new guanylhydrazone derivative as a potential acetylcholinesterase inhibitor for Alzheimer's disease: Synthesis, molecular docking, biological evaluation and kinetic studies by nuclear magnetic resonance, RSC Adv. 7 (2017) 33944–33952. https://doi.org/10.1039/c7ra04180b.

[133]   J.D. Figueroa-Villar, Design, synthesis, structure, toxicology and *in vitro* testing of three novel agents for Alzheimer's disease, RSC Adv. 7 (2017) 23457–23467. https://doi.org/10.1039/c6ra27042e.

[134] D.C. Ferreira Neto, J. Alencar Lima, J. de Almeida, T.C. Costa França, C. do Nascimento, J.D. Figueroa Villar, New semicarbazones as gorge-spanning ligands of acetylcholinesterase and potential new drugs against Alzheimer's disease: Synthesis, molecular modeling, NMR, and biological evaluation, J. Biomol. Struct. Dyn. 36 (2018) 4099–4113. https://doi.org/10.1080/07391102.2017.1407676.

[135] J. Kong, S. Yu, Fourier transform infrared spectroscopic analysis of protein secondary structures, Acta Biochim. Biophys. Sin. 39 (2007) 549–559. https://doi.org/10.1111/j.1745-7270.2007.00320.x.

[136] B. Shanmuganathan, D. Sheeja Malar, S. Sathya, K. Pandima Devi, Antiaggregation potential of *Padina gymnospora* against the toxic Alzheimer's beta-amyloid peptide 25-35 and cholinesterase inhibitory property of its bioactive compounds, PLoS ONE 10 (2015) e0141708. https://doi.org/10.1371/journal.pone.0141708.

[137] A.N. Syad, K.P. Devi, Assessment of anti-amyloidogenic activity of marine red alga *G. acerosa* against Alzheimer's beta-amyloid peptide 25-35, Neurol. Res. 37 (2015) 14–22. https://doi.org/10.1179/1743132814Y.0000000422.

[138] J. Kuret, C.N. Chirita, E.E. Congdon, T. Kannanayakal, G. Li, M. Necula, H. Yin, Q. Zhong, Pathways of tau fibrillization, Biochim. Biophys. Acta 1739 (2005) 167–178. https://doi.org/10.1016/j.bbadis.2004.06.016.

[139] G. Ramachandran, E.A. Milán-Garcés, J.B. Udgaonkar, M. Puranik, Resonance Raman spectroscopic measurements delineate the structural changes that occur during tau fibril formation, Biochemistry (Mosc.) 53 (2014) 6550–6565. https://doi.org/10.1021/bi500528x.

[140] S. Hossain, M. Hashimoto, M. Katakura, A. Al Mamun, O. Shido, Medicinal value of asiaticoside for Alzheimer's disease as assessed using single-molecule-detection fluorescence correlation spectroscopy, laser-scanning microscopy, transmission electron microscopy, and in silico docking, BMC Complement. Altern. Med. 15 (2015) 118. https://doi.org/10.1186/s12906-015-0620-9.

[141] T. Stark, T. Lieblein, M. Pohland, E. Kalden, P. Freund, R. Zangl, R. Grewal, M. Heilemann, G.P. Eckert, N. Morgner, M.W. Göbel, Peptidomimetics that inhibit and partially reverse the aggregation of $A\beta_{1–42}$, Biochemistry (Mosc.) 56 (2017) 4840–4849. https://doi.org/10.1021/acs.biochem.7b00223.

[142] L.A. Woods, S.E. Radford, A.E. Ashcroft, Advances in ion mobility spectrometry-mass spectrometry reveal key insights into amyloid assembly, Biochim. Biophys. Acta Proteins Proteom. 1834 (2013) 1257–1268. https://doi.org/10.1016/j.bbapap.2012.10.002.

[143] G. Grasso, Mass spectrometry is a multifaceted weapon to be used in the battle against Alzheimer's disease: Amyloid beta peptides and beyond, Mass Spectrom. Rev. 38 (2019) 34–48. https://doi.org/10.1002/mas.21566.

[144] J. Folch, M. Ettcheto, D. Petrov, S. Abad, I. Pedrós, M. Marin, J. Olloquequi, A. Camins, Review of the advances in treatment for Alzheimer disease: Strategies for combating β-amyloid protein, Neurologia 33 (2018) 47–58. https://doi.org/10.1016/j.nrleng.2015.03.019.

[145] C.H. van Dyck, Anti-amyloid-β monoclonal antibodies for Alzheimer's disease: Pitfalls and promise, Biol. Psychiatry 83 (2018) 311–319. https://doi.org/10.1016/j.biopsych.2017.08.010.

[146] A.K. Ghosh, H.L. Osswald, BACE1 (β-secretase) inhibitors for the treatment of Alzheimer's disease, Chem. Soc. Rev. 43 (2014) 6765–6813. https://doi.org/10.1039/C3CS60460H.

[147] Q. Wang, X. Yu, L. Li, J. Zheng, Inhibition of amyloid-β aggregation in Alzheimer's disease, Curr. Pharm. Des. 20 (2014) 1223–1243. https://doi.org/10.2174/13816128113199990068.

[148] K.A. Bruggink, M. Müller, H.B. Kuiperij, M.M. Verbeek, Methods for analysis of amyloid-β aggregates, J. Alzheimer's Dis. 28 (2012) 735–758. https://doi.org/10.3233/JAD-2011-111421.

[149] M. Bartolini, M. Naldi, J. Fiori, F. Valle, F. Biscarini, D.V. Nicolau, V. Andrisano, Kinetic characterization of amyloid-beta 1-42 aggregation with a multimethodological approach, Anal. Biochem. 414 (2011) 215–225. https://doi.org/10.1016/j.ab.2011.03.020.

[150] M. Naldi, J. Fiori, M. Pistolozzi, A.F. Drake, C. Bertucci, R. Wu, K. Mlynarczyk, S. Filipek, A. De Simone, V. Andrisano, Amyloid β-peptide 25-35 self-assembly and its inhibition: a model undecapeptide system to gain atomistic and secondary structure details of the Alzheimer's disease process and treatment, ACS Chem. Neurosci. 3 (2012) 952–962. https://doi.org/10.1021/cn3000982.

[151] J. Fiori, N. Naldi, V. Andrisano, Mass spectrometry as an efficient tool for the characterization of amyloid β peptide 25–35 self-assembly species in aggregation and inhibition studies, Eur. J. Mass Spectrom. 19 (2013) 483–490. https://doi.org/10.1255/ejms.1255.

[152] L.M. Young, J.C. Saunders, R.A. Mahood, C.H. Revill, R.J. Foster, L.H. Tu, D.P. Raleigh, S.E. Radford, A.E. Ashcroft, Screening and classifying small-molecule inhibitors of amyloid formation using ion mobility spectrometry-mass spectrometry, Nature Chem. 7 (2015) 73–81. https://doi.org/10.1038/nchem.2129.

[153] C. Bleiholder, M.T. Bowers, The solution assembly of biological molecules using ion mobility methods: From amino acids to amyloid β-protein, Annu. Rev. Anal. Chem. 10 (2017) 365–386. https://doi.org/10.1146/annurev-anchem-071114-040304.

[154] C.E. Eyers, M. Vonderach, S. Ferries, K. Jeacock, P.A. Eyers, Understanding protein–drug interactions using ion mobility–mass spectrometry, Curr. Opin. Chem. Biol. 42 (2018) 167–176. https://doi.org/10.1016/J.CBPA.2017.12.013.

[155] M.A. Downey, M.J. Giammona, C.A. Lang, S.K. Buratto, A. Singh, M.T. Bowers, Inhibiting and remodeling toxic amyloid-beta oligomer formation using a computationally designed drug molecule that targets Alzheimer's disease, J. Am. Soc. Mass Spectrom. 30 (2019) 85–93. https://doi.org/10.1007/s13361-018-1975-1.

[156] A.E. Ashcroft, Mass spectrometry and the amyloid problem – how far can we go in the gas phase?, J. Am. Soc. Mass Spectrom. 21 (2010) 1087–1096. https://doi.org/10.1016/j.jasms.2010.02.026.

[157] Y. Gong, L. Chang, K.L. Viola, P.N. Lacor, M.P. Lambert, C.E. Finch, G.A. Krafft, W.L. Klein, Alzheimer's disease-affected brain: Presence of oligomeric A ligands (ADDLs) suggests a molecular basis for reversible memory loss, Proc. Natl. Acad. Sci. U.S.A. 100 (2003) 10417–10422. https://doi.org/10.1073/pnas.1834302100.

[158] S.L. Bernstein, N.F. Dupuis, N.D. Lazo, T. Wyttenbach, M.M. Condron, G. Bitan, D.B. Teplow, J.-E. Shea, B.T. Ruotolo, C.V. Robinson, M.T. Bowers, Amyloid-β protein oligomerization and the importance of tetramers and dodecamers in the aetiology of Alzheimer's disease, Nature Chem. 1 (2009) 326–331. https://doi.org/10.1038/nchem.247.

[159] N.J. Economou, M.J. Giammona, T.D. Do, X. Zheng, D.B. Teplow, S.K. Buratto, M.T. Bowers, Amyloid β-protein assembly and Alzheimer's disease: Dodecamers of Aβ42, but not of Aβ40, seed fibril formation, J. Am. Chem. Soc. 138 (2016) 1772–1775. https://doi.org/10.1021/jacs.5b11913.

[160] X. Zheng, D. Liu, F.-G. Klärner, T. Schrader, G. Bitan, M.T. Bowers, Amyloid β-protein assembly: The effect of molecular tweezers CLR01 and CLR03, J. Phys. Chem. B 119 (2015) 4831–4841. https://doi.org/10.1021/acs.jpcb.5b00692.

[161] X. Zheng, C. Wu, D. Liu, H. Li, G. Bitan, J.-e. Shea, M.T. Bowers, Mechanism of *C*-terminal fragments of amyloid β-protein as Aβ inhibitors: Do *C*-terminal interactions play a key role in their inhibitory activity?, J. Phys. Chem. B 120 (2016) 1615–1623. https://doi.org/10.1021/acs.jpcb.5b08177.

[162] M. Cernescu, T. Stark, E. Kalden, C. Kurz, K. Leuner, T. Deller, M. Göbel, G.P. Eckert, B. Brutschy, Laser-induced liquid bead ion desorption mass spectrometry: An approach to precisely monitor the oligomerization of the β-amyloid peptide, Anal. Chem. 84 (2012) 5276–5284. https://doi.org/10.1021/ac300258m.

[163] H.J. Maple, R.A. Garlish, L. Rigau-Roca, J. Porter, I. Whitcombe, C.E. Prosser, J. Kennedy, A.J. Henry, R.J. Taylor, M.P. Crump, J. Crosby, Automated protein–ligand interaction screening by mass spectrometry, J. Med. Chem. 55 (2012) 837–851. https://doi.org/10.1021/jm201347k.

[164] L.M. Young, J.C. Saunders, R.A. Mahood, C.H. Revill, R.J. Foster, A.E. Ashcroft, S.E. Radford, ESI-IMS–MS: A method for rapid analysis of protein aggregation and its inhibition by small molecules, Methods 95 (2016) 62–69. https://doi.org/10.1016/j.ymeth.2015.05.017.

[165] K. Ishii, M. Noda, S. Uchiyama, Mass spectrometric analysis of protein–ligand interactions, Biophys. Physicobiol. 13 (2016) 87–95. https://doi.org/10.2142/biophysico.13.0_87.

[166] T. Liu, T.M. Marcinko, P.A. Kiefer, R.W. Vachet, Using covalent labeling and mass spectrometry to study protein binding sites of amyloid inhibiting molecules, Anal. Chem. 89 (2017) 11583–11591. https://doi.org/10.1021/acs.analchem.7b02915.

[167] V. Minicozzi, R. Chiaraluce, V. Consalvi, C. Giordano, C. Narcisi, P. Punzi, G.C. Rossi, S. Morante, Computational and experimental studies on β-sheet breakers targeting Aβ$_{1\text{-}40}$ fibrils, J. Biol. Chem. 289 (2014) 11242–11252. https://doi.org/10.1074/jbc.M113.537472.

[168] L. Lu, H.-j. Zhong, M. Wang, S.-l. Ho, H.-w. Li, C.-H. Leung, D.-L. Ma, Inhibition of beta-amyloid fibrillation by luminescent iridium(III) complex probes, Sci. Rep. 5 (2015) 14619. https://doi.org/10.1038/srep14619.

[169] V. Oliveri, F. Bellia, G. Vecchio, Cyclodextrin 3-functionalized with 8-hydroxyquinoline as an antioxidant inhibitor of metal-induced amyloid aggregation, ChemPlusChem 80 (2015) 762–770. https://doi.org/10.1002/cplu.201402450.

[170] E.N. Cline, A. Das, M.A. Bicca, S.N. Mohammad, L.F. Schachner, J.M. Kamel, N. DiNunno, A. Weng, J.D. Paschall, R.L. Bu, F.M. Khan, M.G. Rollins, A.N. Ives, G. Shekhawat, N. Nunes-Tavares, F.G. de Mello, P.D. Compton, N.L. Kelleher, W.L. Klein, A novel crosslinking protocol stabilizes amyloid β oligomers capable of inducing Alzheimer's-associated pathologies, J. Neurochem. 148 (2019) 822–836. https://doi.org/10.1111/jnc.14647.

[171] W. Hoffmann, G. von Helden, K. Pagel, Ion mobility-mass spectrometry and orthogonal gas-phase techniques to study amyloid formation and inhibition, Curr. Opin. Struct. Biol. 46 (2017) 7–15. https://doi.org/10.1016/j.sbi.2017.03.002.

[172] P. Aisen, S. Gauthier, B. Vellas, R. Briand, D. Saumier, J. Laurin, D. Garceau, Alzhemed: A potential treatment for Alzheimers disease, Curr. Alzheimer Res. 4 (2007) 473–478. https://doi.org/10.2174/156720507781788882.

[173] M. Necula, R. Kayed, S. Milton, C.G. Glabe, Small molecule inhibitors of aggregation indicate that amyloid β oligomerization and fibrillization pathways are independent and distinct, J. Biol. Chem. 282 (2007) 10311–10324. https://doi.org/10.1074/jbc.M608207200.

[174] K. Andrich, J. Bieschke, The effect of (−)-epigallo-catechin-(3)-gallate on amyloidogenic proteins suggests a common mechanism, Adv. Exp. Med. Biol. 863 (2015) 139–161. https://doi.org/10.1007/978-3-319-18365-7_7.

[175] J. Nunes, C. Charneira, J. Morello, J. Rodrigues, S.A. Pereira, A.M.M. Antunes, Mass spectrometry-based methodologies for targeted and untargeted identification of protein covalent adducts (adductomics): Current status and challenges, High Throughput 8 (2019) 9. https://doi.org/10.3390/ht8020009.

[176] J. Fiori, M. Naldi, M. Bartolini, V. Andrisano, Disclosure of a fundamental clue for the elucidation of the myricetin mechanism of action as amyloid aggregation inhibitor by mass spectrometry, Electrophoresis 33 (2012) 3380–3386. https://doi.org/10.1002/elps.201200186.

[177] A. Taniguchi, D. Sasaki, A. Shiohara, T. Iwatsubo, T. Tomita, Y. Sohma, M. Kanai, Attenuation of the aggregation and neurotoxicity of amyloid-β peptides by catalytic photooxygenation, Angew. Chem. Int. Ed. Engl. 53 (2014) 1382–1385. https://doi.org/10.1002/anie.201308001.

[178] A. Albreht, I. Vovk, J. Mavri, J. Marco-Contelles, R.R. Ramsay, Evidence for a cyanine link between propargylamine drugs and monoamine oxidase clarifies the inactivation mechanism, Front. Chem. 6 (2018) 1–11. https://doi.org/10.3389/fchem.2018.00169.

[179] A. Dey, R. Bhattacharya, A. Mukherjee, D.K. Pandey, Natural products against Alzheimer's disease: Pharmaco-therapeutics and biotechnological interventions, Biotechnol. Adv. 35 (2017) 178–216. https://doi.org/10.1016/j.biotechadv.2016.12.005.

[180] T.T. Bui, T.H. Nguyen, Natural product for the treatment of Alzheimer's disease, J. Basic Clin. Physiol. Pharmacol. 28 (2017) 413–423. https://doi.org/10.1515/jbcpp-2016-0147.

[181] X. Wu, H. Cai, L. Pan, G. Cui, F. Qin, Y. Li, Z. Cai, Small molecule natural products and Alzheimer's disease, Curr. Top. Med. Chem. 19 (2019) 187–204. https://doi.org/10.2174/1568026619666190201153257.

[182] L. Wang, Y. Zhao, Y. Zhang, T. Zhang, J. Kool, G.W. Somsen, Q. Wang, Z. Jiang, Online screening of acetylcholinesterase inhibitors in natural products using monolith-based immobilized capillary enzyme reactors combined with liquid chromatography-mass spectrometry, J. Chromatogr. A 1563 (2018) 135–143. https://doi.org/10.1016/j.chroma.2018.05.069.

[183] R. Zhuo, H. Liu, N. Liu, Y. Wang, Ligand fishing: A remarkable strategy for discovering bioactive compounds from complex mixture of natural products, Molecules 21 (2016) 1516. https://doi.org/10.3390/molecules21111516.

[184] G.F. Wu, X.L. Jiang, Y.Z. Gong, Y.D. Hu, X.L. Bai, X. Liao, Ligand fishing of anti-neurodegenerative components from *Lonicera japonica* using magnetic nanoparticles immobilised with monoamine oxidase B, J. Sep. Sci. 42 (2019) 1289–1298. https://doi.org/10.1002/jssc.201801255.

[185] Y. Zhang, Q. Wang, R. Liu, H. Zhou, J. Crommen, R. Moaddel, Z. Jiang, T. Zhang, Rapid screening and identification of monoamine oxidase-A inhibitors from corydalis rhizome using enzyme-immobilized magnetic beads based method, J. Chromatogr. A 1592 (2019) 1–8. https://doi.org/10.1016/j.chroma.2019.01.062.

[186] S. Sun, B.C. Buer, E.N.G. Marsh, R.T. Kennedy, A label-free Sirtuin 1 assay based on droplet-electrospray ionization mass spectrometry, Anal. Methods 8 (2016) 3458–3465. https://doi.org/10.1039/C6AY00698A.

[187] L. Peng, Z. Rong, H. Wang, B. Shao, L. Kang, H. Qi, H. Chen, A novel assay to determine acetylcholinesterase activity: The application potential for screening of drugs against Alzheimer's disease, Biomed. Chromatogr. 31 (2017) 2–7. https://doi.org/10.1002/bmc.3971.

[188] A. De Simone, J. Fiori, M. Naldi, A. D'Urzo, V. Tumiatti, A. Milelli, V. Andrisano, Application of an ESI-QTOF method for the detailed characterization of GSK-3β inhibitors, J. Pharm. Biomed. Anal. 144 (2017) 159–166. https://doi.org/10.1016/j.jpba.2017.02.036.

[189] J. Schejbal, L. Slezáčková, R. Řemínek, Z. Glatz, A capillary electrophoresis-mass spectrometry based method for the screening of β-secretase inhibitors as potential Alzheimer's disease therapeutics, J. Chromatogr. A 1487 (2017) 235–241. https://doi.org/10.1016/j.chroma.2017.01.057.

[190] M. Machálková, J. Schejbal, Z. Glatz, J. Preisler, A label-free MALDI TOF MS-based method for studying the kinetics and inhibitor screening of the Alzheimer's disease drug target β-secretase, Anal. Bioanal. Chem. 410 (2018) 7441–7448. https://doi.org/10.1007/s00216-018-1354-6.

[191] C.A. Scarff, M.J.G. Fuller, R.F. Thompson, M.G. Iadaza, Variations on negative stain electron microscopy methods: Tools for tackling challenging systems, J. Vis. Exp. 132 (2018) 57199. https://doi.org/10.3791/57199.

[192] S.H. Omar, C.J. Scott, A.S. Hamlin, H.K. Obied, Olive biophenols reduces Alzheimer's pathology in SH-SY5Y cells and APPswe mice, Int. J. Mol. Sci. 20 (2018) 125. https://doi.org/10.3390/ijms20010125.

[193] M.K. Siddiqi, P. Alam, S. Malik, N. Majid, S.K. Chaturvedi, S. Rajan, M.R. Ajmal, M.V. Khan, V.N. Uversky, R.H. Khan, Stabilizing proteins to prevent conformational changes required for amyloid fibril formation, J. Cell. Biochem. 120 (2018) 2642–2656. https://doi.org/10.1002/jcb.27576.

[194] P. Alam, M.K. Siddiqi, S. Malik, S.K. Chaturvedi, M. Uddin, R.H. Khan, Elucidating the inhibitory potential of vitamin A against fibrillation and amyloid associated cytotoxicity, Int. J. Biol. Macromol. 129 (2019) 333–338. https://doi.org/10.1016/j.ijbiomac.2019.01.134.

[195] F. Bisceglia, F. Seghetti, M. Serra, M. Zusso, S. Gervasoni, L. Verga, G. Vistoli, C. Lanni, M. Catanzaro, E. De Lorenzi, F. Belluti, Prenylated curcumin analogues as multipotent tools to tackle Alzheimer's disease, ACS Chem. Neurosci. 10 (2019) 1420–1433. https://doi.org/10.1021/acschemneuro.8b00463.

[196] Q. Huang, Q. Zhao, J. Peng, Y. Yu, C. Wang, Y. Zou, Y. Su, L. Zhu, C. Wang, Y. Yang, Peptide-polyphenol (KLVFF/EGCG) binary modulators for inhibiting aggregation and neurotoxicity of amyloid-β peptide, ACS Omega 4 (2019) 4233–4242. https://doi.org/10.1021/acsomega.8b02797.

[197] A. Kaur, S. Mann, N. Priyadarshi, B. Goyal, N.K. Singhal, D. Goyal, Multi-target-directed triazole derivatives as promising agents for the treatment of Alzheimer's disease, Bioorg. Chem. 87 (2019) 572–584. https://doi.org/10.1016/j.bioorg.2019.03.058.

[198] S. Millan, L. Satish, K. Bera, H. Sahoo, Binding and inhibitory effect of the food colorants Sunset Yellow and Ponceau 4R on amyloid fibrillation of lysozyme, New J. Chem. 43 (2019) 3956–3968. https://doi.org/10.1039/c8nj05827j.

[199] K. Pradhan, G. Das, V. Gupta, P. Mondal, S. Barman, J. Khan, S. Ghosh, Discovery of neuroregenerative peptoid from amphibian neuropeptide that inhibits amyloid-β toxicity and crosses blood-brain barrier, ACS Chem. Neurosci. 10 (2019) 1355–1368. https://doi.org/10.1021/acschemneuro.8b00427.

[200] J. Sun, G. Jiang, H. Shigemori, Inhibitory activity on amyloid aggregation of rosmarinic acid and its substructures from *Isodon japonicus*, Nat. Prod. Commun. 14 (2019) 1–5. https://doi.org/10.1177/1934578X19843039.

[201] G. Tin, T. Mohamed, A. Shakeri, A.T. Pham, P.P.N. Rao, Interactions of selective serotonin reuptake inhibitors with β-amyloid, ACS Chem. Neurosci. 10 (2019) 226–234. https://doi.org/10.1021/acschemneuro.8b00160.

[202] T. Umar, S. Shalini, M.K. Raza, S. Gusain, J. Kumar, P. Seth, M. Tiwari, N. Hoda, A multifunctional therapeutic approach: Synthesis, biological evaluation, crystal structure and molecular docking of diversified 1*H*-pyrazolo[3,4-b]pyridine derivatives against Alzheimer's disease, Eur. J. Med. Chem. 175 (2019) 2–19. https://doi.org/10.1016/j.ejmech.2019.04.038.

[203] T. Umar, S. Gusain, M.K. Raza, S. Shalini, J. Kumar, M. Tiwari, N. Hoda, Naphthalene-triazolopyrimidine hybrid compounds as potential multifunctional anti-Alzheimer's agents, Bioorg. Med. Chem. 27 (2019) 3156–3166. https://doi.org/10.1016/j.bmc.2019.06.004.

[204] J. Wang, K. Wang, Z. Zhu, Y. He, C. Zhang, Z. Guo, X. Wang, Inhibition of metal-induced amyloid β-peptide aggregation by a blood-brain barrier permeable silica-cyclen nanochelator, RSC Adv. 9 (2019) 14126–14131. https://doi.org/10.1039/c9ra02358e.

[205] Q. Zhan, X. Shi, T. Wang, J. Hu, J. Zhou, L. Zhou, S. Wei, Design and synthesis of thymine modified phthalocyanine for Aβ protofibrils photodegradation and Aβ peptide aggregation inhibition, Talanta 191 (2019) 27–38. https://doi.org/10.1016/j.talanta.2018.08.037.

[206] M. Frenkel-Pinter, S. Tal, R. Scherzer-Attali, M. Abu-Hussien, I. Alyagor, T. Eisenbaum, E. Gazit, D. Segal, Naphthoquinone-tryptophan hybrid inhibits aggregation of the tau-derived peptide PHF6 and reduces neurotoxicity, J. Alzheimer's Dis. 51 (2016) 165–178. https://doi.org/10.3233/JAD-150927.

[207] M. Frenkel-Pinter, S. Tal, R. Scherzer-Attali, M. Abu-Hussien, I. Alyagor, T. Eisenbaum, E. Gazit, D. Segal, Cl-NQTrp alleviates tauopathy symptoms in a model organism through the inhibition of tau aggregation-engendered toxicity, Neurodegener. Dis. 17 (2017) 73–82. https://doi.org/10.1159/000448518.

[208] S. Rafiee, K. Asadollahi, G. Riazi, S. Ahmadian, A.A. Saboury, Vitamin B12 inhibits tau fibrillization via binding to cysteine residues of tau, ACS Chem. Neurosci. 8 (2017) 2676–2682. https://doi.org/10.1021/acschemneuro.7b00230.

[209] J.S. Rane, P. Bhaumik, D. Panda, Curcumin inhibits tau aggregation and disintegrates preformed tau filaments *in vitro*, J. Alzheimer's Dis. 60 (2017) 999–1014. https://doi.org/10.3233/JAD-170351.

[210] Y.K. Al-Hilaly, S.J. Pollack, J.E. Rickard, M. Simpson, A.C. Raulin, T. Baddeley, P. Schellenberger, J.M.D. Storey, C.R. Harrington, C.M. Wischik, L.C. Serpell, Cysteine-independent inhibition of Alzheimer's disease-like paired

helical filament assembly by leuco-methylthioninium (LMT), J. Mol. Biol. 430 (2018) 4119–4131. https://doi.org/10.1016/j.jmb.2018.08.010.

[211] V.G. KrishnaKumar, A. Paul, E. Gazit, D. Segal, Mechanistic insights into remodeled tau-derived PHF6 peptide fibrils by naphthoquinone-tryptophan hybrids, Sci. Rep. 8 (2018) 71. https://doi.org/10.1038/s41598-017-18443-2.

[212] C.J. Huseby, J. Kuret, Analyzing tau aggregation with electron microscopy, Methods Mol. Biol. 1345 (2016) 101–112. https://doi.org/10.1007/978-1-4939-2978-8_7.

[213] N. Nanavaty, L. Lin, S.H. Hinckley, J. Kuret, Detection and quantification methods for fibrillar products of *in vitro* tau aggregation assays, Methods Mol. Biol. 1523 (2017) 101–111. https://doi.org/10.1007/978-1-4939-6598-4_6.

[214] P. Ganguly, T.D. Do, L. Larini, N.E. LaPointe, A.J. Sercel, M.F. Shade, S.C. Feinstein, M.T. Bowers, J.E. Shea, Tau assembly: The dominant role of PHF6 (VQIVYK) in microtubule binding region repeat R3, J. Phys. Chem. B 119 (2015) 4582–4593. https://doi.org/10.1021/acs.jpcb.5b00175.

[215] D. Pinkaew, C. Changtam, C. Tocharus, S. Thummayot, A. Suksamrarn, J. Tocharus, Di-*O*-demethylcurcumin protects SK-N-SH cells against mitochondrial and endoplasmic reticulum-mediated apoptotic cell death induced by $A\beta_{25-35}$, Neurochem. Int. 80 (2015) 110–119. https://doi.org/10.1016/j.neuint.2014.10.008.

[216] H. Xiao, L. Ma, Y. Li, X. Wu, F. Yuan, Flavones from vitis vinifera L inhibits $A\beta_{25-35}$-induced apoptosis in PC12 cells, Int. J. Clin. Exp. Med. 10 (2017) 8866–8874.

[217] X.H. Ma, W.J. Duan, Y.S. Mo, J.L. Chen, S. Li, W. Zhao, L. Yang, S.Q. Mi, X.L. Mao, H. Wang, Q. Wang, Neuroprotective effect of paeoniflorin on okadaic acid-induced tau hyperphosphorylation via calpain/Akt/GSK-3β pathway in SH-SY5Y cells, Brain Res. 1690 (2018) 1–11. https://doi.org/10.1016/j.brainres.2018.03.022.

[218] C. Gao, Y. Liu, Y. Jiang, J. Ding, L. Li, Geniposide ameliorates learning memory deficits, reduces tau phosphorylation and decreases apoptosis via GSK3β pathway in streptozotocin-induced alzheimer rat model, Brain Pathol. 24 (2014) 261–269. https://doi.org/10.1111/bpa.12116.

[219] A. Zaky, A. Bassiouny, M. Farghaly, B.M. El-Sabaa, A combination of resveratrol and curcumin is effective against aluminum chloride-induced neuroinflammation in rats, J. Alzheimer's Dis. 60 (2017) S221–S235. https://doi.org/10.3233/JAD-161115.

[220] E.R. Fischer, B.T. Hansen, V. Nair, F.H. Hoyt, D.W. Dorward, Scanning electron microscopy, Curr. Protoc. Microbiol. 25 (2012) 2B.2.1–2B.2.47. https://doi.org/10.1002/9780471729259.mc02b02s25.

[221] J.S. Ploem, Laser scanning fluorescence microscopy, Appl. Opt. 26 (1987) 3226–3231. https://doi.org/10.1364/AO.26.003226.

[222] B. Shanmuganathan, V. Suryanarayanan, S. Sathya, M. Narenkumar, S.K. Singh, K. Ruckmani, K. Pandima Devi, Anti-amyloidogenic and anti-apoptotic effect of α-bisabolol against Aβ induced neurotoxicity in PC12 cells, Eur. J. Med. Chem. 143 (2018) 1196–1207. https://doi.org/10.1016/j.ejmech.2017.10.017.

[223] S.A. Nisha, K.P. Devi, *Gelidiella acerosa* protects against Aβ 25–35-induced toxicity and memory impairment in Swiss Albino mice: An *in vivo* report, Pharm. Biol. 55 (2017) 1423–1435. https://doi.org/10.1080/13880209.2017.1302967.

[224] S.H. Cohen, M.T. Bray, M.L. Lightbody, Atomic Force Microscopy/Scanning Tunneling Microscopy, Plenum Press, New York, 1994.

[225] U. Maver, T. Velnar, M. Gaberšček, O. Planinšek, M. Finšga, Recent progressive use of atomic force microscopy in biomedical applications, Trends Anal. Chem. 80 (2016) 96–111. https://doi.org/10.1016/j.trac.2016.03.014.

[226] S.B. Bansode, A.K. Jana, K.B. Batkulwar, S.D. Warkad, R.S. Joshi, N. Sengupta, M.J. Kulkarni, Molecular investigations of protriptyline as a multi-target directed ligand in Alzheimer's disease, PLoS ONE 9 (2014) e105196. https://doi.org/10.1371/journal.pone.0105196.

[227] L. Fang, X. Fang, S. Gou, A. Lupp, I. Lenhardt, Y. Sun, Z. Huang, Y. Chen, Y. Zhang, C. Fleck, Design, synthesis and biological evaluation of D-ring opened galantamine analogs as multifunctional anti-Alzheimer agents, Eur. J. Med. Chem. 76 (2014) 376–386. https://doi.org/10.1016/j.ejmech.2014.02.035.

[228] Z. Fu, D. Aucoin, M. Ahmed, M. Ziliox, W.E. Van Nostrand, S.O. Smith, Capping of Aβ42 oligomers by small molecule inhibitors, Biochemistry (Mosc.) 53 (2014) 7893–7903. https://doi.org/10.1021/bi500910b.

[229] F.T. Hane, B.Y. Lee, A. Petoyan, A. Rauk, Z. Leonenko, Testing synthetic amyloid-β aggregation inhibitor using single molecule atomic force spectroscopy, Biosens. Bioelectron. 54 (2014) 492–498. https://doi.org/10.1016/j.bios.2013.10.060.

[230] V.B. Kovalska, M.Y. Losytskyy, O.A. Varzatskii, V.V. Cherepanov, Y.Z. Voloshin, A.A. Mokhir, S.M. Yarmoluk, S.V. Volkov, Study of anti-fibrillogenic activity of iron(II) clathrochelates, Bioorg. Med. Chem. 22 (2014) 1883–1888. https://doi.org/10.1016/j.bmc.2014.01.048.

[231] P. Wang, W. Liao, J. Fang, Q. Liu, J. Yao, M. Hu, K. Ding, A glucan isolated from flowers of *Lonicera japonica* Thunb. inhibits aggregation and neurotoxicity of Aβ42, Carbohydr. Polym. 110 (2014) 142–147. https://doi.org/10.1016/j.carbpol.2014.03.060.

[232] Q. Wang, G. Liang, M. Zhang, J. Zhao, K. Patel, X. Yu, C. Zhao, B. Ding, G. Zhang, F. Zhou, J. Zheng, De novo design of self-assembled hexapeptides as β-amyloid (Aβ) peptide inhibitors, ACS Chem. Neurosci. 5 (2014) 972–981. https://doi.org/10.1021/cn500165s.

[233] L. Xie, Y. Luo, D. Lin, W. Xi, X. Yang, G. Wei, The molecular mechanism of fullerene-inhibited aggregation of Alzheimer's β-amyloid peptide fragment, Nanoscale 6 (2014) 9752–9762. https://doi.org/10.1039/c4nr01005a.

[234] S. Ghimire Gautam, M. Komatsu, K. Nishigaki, Strong inhibition of beta-amyloid peptide aggregation realized by two-steps evolved peptides, Chem. Biol. Drug Des. 85 (2015) 356–368. https://doi.org/10.1111/cbdd.12400.

[235] H. Ramshini, M. mohammad-zadeh, A. Ebrahim-Habibi, Inhibition of amyloid fibril formation and cytotoxicity by a chemical analog of curcumin as a stable inhibitor, Int. J. Biol. Macromol. 78 (2015) 396–404. https://doi.org/10.1016/j.ijbiomac.2015.04.038.

[236] Q. Van Vuong, Bednarikova, Z., Antosova, A., Huy, P.D.Q., Siposova, K., Tuan, N.A., Li, M.S., Gazova, Z., Inhibition of insulin amyloid fibrillization by glyco-acridines: An *in vitro* and *in silico* study, MedChemComm 6 (2015) 810–822. https://doi.org/10.1039/c5md00004a.

[237] Z. Bednarikova, P.D. Huy, M.M. Mocanu, D. Fedunova, M.S. Li, Z. Gazova, Fullerenol $C_{60}(OH)_{16}$ prevents amyloid fibrillization of $A\beta_{40}$ – *in vitro* and *in silico* approach, Phys. Chem. Chem. Phys. 18 (2016) 18855–18867. https://doi.org/10.1039/c6cp00901h.

[238] S. Chakraborty, J. Bandyopadhyay, S. Basu, Multi-target screening mines hesperidin as a multi-potent inhibitor: Implication in Alzheimer's disease therapeutics, Eur. J. Med. Chem. 121 (2016) 810–822. https://doi.org/10.1016/j.ejmech.2016.03.057.

[239] W. Lee, Kim, I., Lee, S.W., Lee, H., Lee, G., Kim, S., Lee, S.W., Yoon, D.S., Quantifying L-ascorbic acid-driven inhibitory effect on amyloid fibrillation, Macromol. Res. 24 (2016) 868–873. https://doi.org/10.1007/s13233-016-4126-1.

[240] L. Niu, L. Liu, W. Xi, Q. Han, Q. Li, Y. Yu, Q. Huang, F. Qu, M. Xu, Y. Li, H. Du, R. Yang, J. Cramer, K.V. Gothelf, M. Dong, F. Besenbacher, Q. Zeng, C. Wang, G. Wei, Y. Yang, Synergistic inhibitory effect of peptide-organic coassemblies on amyloid aggregation, ACS Nano 10 (2016) 4143–4153. https://doi.org/10.1021/acsnano.5b07396.

[241] A. Cornejo, F. Aguilar Sandoval, L. Caballero, L. Machuca, P. Muñoz, J. Caballero, G. Perry, A. Ardiles, C. Areche, F. Melo, Rosmarinic acid prevents fibrillization and diminishes vibrational modes associated to β sheet in tau protein linked to Alzheimer's disease, J. Enzyme Inhib. Med. Chem. 32 (2017) 945–953. https://doi.org/10.1080/14756366.2017.1347783.

[242] E. Ferrari, R. Benassi, M. Saladini, G. Orteca, Z. Gazova, K. Siposova, *In vitro* study on potential pharmacological activity of curcumin analogues and their copper complexes, Chem. Biol. Drug Des. 89 (2017) 411–419. https://doi.org/10.1111/cbdd.12847.

[243] X. Han, J. Park, W. Wu, A. Malagon, L. Wang, E. Vargas, A. Wikramanayake, K.N. Houk, R.M. Leblanc, A resorcinarene for inhibition of Aβ fibrillation, Chem. Sci. 8 (2017) 2003–2009. https://doi.org/10.1039/c6sc04854d.

[244] P.D.Q. Huy, N.Q. Thai, Z. Bednarikova, L.H. Phuc, H.Q. Linh, Z. Gazova, M.S. Li, Bexarotene does not clear amyloid beta plaques but delays fibril growth: Molecular mechanisms, ACS Chem. Neurosci. 8 (2017) 1960–1969. https://doi.org/10.1021/acschemneuro.7b00107.

[245] M.F.M. Sciacca, V. Romanucci, A. Zarrelli, I. Monaco, F. Lolicato, N. Spinella, C. Galati, G. Grasso, L. D'Urso, M. Romeo, L. Diomede, M. Salmona, C. Bongiorno, G. Di Fabio, C. La Rosa, D. Milardi, Inhibition of Aβ amyloid growth and toxicity by silybins: The crucial role of stereochemistry, ACS Chem. Neurosci. 8 (2017) 1767–1778. https://doi.org/10.1021/acschemneuro.7b00110.

[246] L.Y. Bao, S.J. Hao, S.F. Xi, X. Yan, H.X. Zhang, R. Shen, Z.G. Gu, Chiral supramolecular coordination cages as high-performance inhibitors against amyloid-β aggregation, Chem. Commun. 54 (2018) 8725–8728. https://doi.org/10.1039/c8cc04913k.

[247] S. Chakraborty, Rakshit, J., Bandyopadhyay, J., Basu, S., Multi-functional neuroprotective activity of neohesperidin dihydrochalcone: A novel scaffold for Alzheimer's disease therapeutics identified via drug repurposing screening, New J. Chem. 42 (2018) 11755–11769. https://doi.org/10.1039/c8nj00853a.

[248] A. Hiremathad, K. Chand, L. Tolayan, Rajeshwari, R.S. Keri, A.R. Esteves, S.M. Cardoso, S. Chaves, M.A. Santos, Hydroxypyridinone-benzofuran hybrids with potential protective roles for Alzheimer´s disease therapy, J. Inorg. Biochem. 179 (2018) 82–96. https://doi.org/10.1016/j.jinorgbio.2017.11.015.

[249] W. Lee, S.W. Lee, G. Lee, D.S. Yoon, Atomic force microscopy analysis of EPPS-driven degradation and reformation of amyloid-β aggregates, J. Alzheimer's Dis. Rep. 2 (2018) 41–49. https://doi.org/10.3233/ADR-170024.

[250] Q. Liu, J. Fang, P. Wang, Z. Du, Y. Li, S. Wang, K. Ding, Characterization of a pectin from Lonicera japonica Thunb. and its inhibition effect on Aβ, Int. J. Biol. Macromol. 107 (2018) 112–120. https://doi.org/10.1016/j.ijbiomac.2017.08.154.

[251] H. Zhang, X. Dong, F. Liu, J. Zheng, Y. Sun, Ac-LVFFARK-NH$_2$ conjugation to β-cyclodextrin exhibits significantly enhanced performance on inhibiting amyloid β-protein fibrillogenesis and cytotoxicity, Biophys. Chem. 235 (2018) 40–47. https://doi.org/10.1016/j.bpc.2018.02.002.

[252] P. Sharma, A. Tripathi, P.N. Tripathi, S.K. Prajapati, A. Seth, M.K. Tripathi, P. Srivastava, V. Tiwari, S. Krishnamurthy, S.K. Shrivastava, Design and development of multitarget-directed *N*-benzylpiperidine analogs as potential candidates for the treatment of Alzheimer's disease, Eur. J. Med. Chem. 167 (2019) 510–524. https://doi.org/10.1016/j.ejmech.2019.02.030.

[253] K. Siposova, T. Kozar, V. Huntosova, S. Tomkova, A. Musatov, Inhibition of amyloid fibril formation and disassembly of pre-formed fibrils by natural polyphenol rottlerin, Biochim. Biophys. Acta Proteins Proteom. 1867 (2019) 259–274. https://doi.org/10.1016/j.bbapap.2018.10.002.

[254] F. Lo Cascio, R. Kayed, Azure C targets and modulates toxic tau oligomers, ACS Chem. Neurosci. 9 (2018) 1317–1326. https://doi.org/10.1021/acschemneuro.7b00501.

[255] Y. Soeda, M. Saito, S. Maeda, K. Ishida, A. Nakamura, S. Kojima, A. Takashima, Methylene Blue inhibits formation of tau fibrils but not of granular tau oligomers: A plausible key to understanding failure of a clinical trial for Alzheimer's disease, J. Alzheimer's Dis. 68 (2019) 1677–1686. https://doi.org/10.3233/JAD-181001.

[256] L. Lunven, H. Bonnet, S. Yahiaoui, W. Yi, L. Da Costa, M. Peuchmaur, A. Boumendjel, S. Chierici, Disruption of fibers from the tau model AcPHF6 by naturally occurring aurones and synthetic analogues, ACS Chem. Neurosci. 7 (2016) 995–1003. https://doi.org/10.1021/acschemneuro.6b00102.

[257] H.T.T. Phan, K. Samarat, Y. Takamura, A.F. Azo-Oussou, Y. Nakazono, M.C. Vestergaard, Polyphenols modulate Alzheimer's amyloid beta aggregation in a structure-dependent manner, Nutrients 11 (2019) 756. https://doi.org/10.3390/nu11040756.

[258] M.J. Guerrero-Muñoz, J. Gerson, D.L. Castillo-Carranza, Tau oligomers: The toxic player at synapses in Alzheimer's disease, Front Cell Neurosci 9 (2015) 464. https://doi.org/10.3389/fncel.2015.00464.

[259] S.J. Lee, E. Nam, H.J. Lee, M.G. Savelieff, M.H. Lim, Towards an understanding of amyloid-β oligomers: Characterization, toxicity mechanisms, and inhibitors, Chem. Soc. Rev. 46 (2017) 310–323. https://doi.org/10.1039/c6cs00731g.

[260] T. Watanabe-Nakayama, K. Ono, M. Itami, R. Takahashi, D.B. Teplow, M. Yamada, High-speed atomic force microscopy reveals structural dynamics of amyloid β$_{1-42}$ aggregates, Proc Natl Acad Sci U S A 113 (2016) 5835–5840. https://doi.org/10.1073/pnas.1524807113.

[261] S. Banerjee, Z. Sun, E.Y. Hayden, D.B. Teplow, Y.L. Lyubchenko, Nanoscale dynamics of amyloid β-42 oligomers as revealed by high-speed atomic force microscopy, ACS Nano 11 (2017) 12202–12209. https://doi.org/10.1021/acsnano.7b05434.